2017

Developing a hydrological monitoring program for ponds in Wapusk National Park, Manitoba, using water isotope tracers

Stephanie Roy
royx9290@mylaurier.ca

Developing a hydrological monitoring program for ponds in Wapusk National Park, Manitoba, using water isotope tracers

By

Stephanie J. Roy

Honours BA Geography, Wilfrid Laurier University, 2014

Thesis

Submitted to the Department of Geography and Environmental Studies

Faculty of Arts

in partial fulfilment of the requirements for the

Master of Science in Geography and Environmental Studies

Wilfrid Laurier University

2017

Abstract

Northern lake-rich landscapes are vulnerable to increases in surface air temperatures and are changing in dynamic ways. Current meteorological records indicate that some of the greatest warming in the past century has occurred in the Hudson Bay Lowlands (HBL). As the HBL is an extensive wetland consisting of hundreds of thousands of shallow lakes and ponds, it is difficult to anticipate the long-term implications that climate change will have on pond water balance. To develop and implement long-term monitoring of hydrological conditions, sampling of pond water isotope composition has occurred during the past six years in Wapusk National Park (WNP), located in the HBL. This research is part of a collaboration among WNP, Wilfrid Laurier University and the University of Waterloo and is designed to establish standard operating procedures that will be incorporated into hydrological monitoring protocols for sampling ponds within the Park.

Previous studies have implemented long-term hydrological monitoring programs in thermokarst landscapes using water isotope tracers. Water isotope tracers are an excellent tool for characterizing spatial and temporal variability of pond water balances. Here, we use water isotope tracers (^{18}O and ^{2}H) on 16 ponds in WNP, northern Manitoba, employed over

a six-year sampling period. Water isotope samples were collected three times each year during 2010 – 2015 (early, mid- and late ice-free season) to evaluate seasonal and annual patterns of pond water balance, and their drivers. An isotope framework based on evaporation pan data was developed to provide reliable and accurate means for interpreting water isotope compositions. A coupled-isotope tracer method was applied to obtain estimates of the isotope composition of input water (δ_I) and evaporation to inflow (E/I) ratios. Results provide insight into meteorological and catchment conditions influencing the seasonal, annual and spatial variability in pond water balance. Generally, δ_I values indicate pond water balances during the monitoring interval are influenced mainly by rainfall. E/I ratios reveal that ponds in the coastal fen and peat plateau ecozone are more influenced by mid-season evaporation and are more susceptible to pond-level drawdown than those in the boreal spruce ecozone. Higher than climate normal precipitation during 2014 and 2015 offset mid-ice-free season evaporation in most ponds. These results indicate that pond hydrological responses to climate change are likely to be complex and are related to catchment characteristics and ice-on and ice-free precipitation amounts. Data from the water isotope framework will be shared with Parks Canada as a tool for future monitoring. Ongoing monitoring will provide key

hydrological metrics for current pond water balance conditions to monitor future responses to climate change.

Acknowledgements

First and foremost I would like to thank the wonderful women who showed me the ropes in the lab and in the field, Hilary White and Lauren MacDonald. Without your knowledge and expertise I would probably be wandering the wetlands of Wapusk National Park. Thank you so much for showing me not only how to collect samples and process them in the lab, but how to find effective research papers and communicate in the language of science. Your understanding and passion in the world of science is truly inspiring. I would also like to thank my supervisor Brent Wolfe for introducing me to the world of water isotopes. You have given me the opportunity to explore parts of the world I may never have gone to and encouraged me to become more independent in my scientific endeavours. A huge thank you to all of the funding sources that made this possible including: Natural Sciences and Engineering Research Council of Canada, the Polar Continental Shelf Program, the Northern Scientific Training Program, and the Churchill Northern Studies Centre. I would like to thank my brother-in-law Erik for providing great helicopter experience and comradery in Churchill. I would also like to thank my parents, Lori and Laurence, and my sisters Carolyn and Michelle for 'going with the flow' as I keep going further and further with

school. Last but not least I would like to thank my partner Aran for being there for me as I worked full time at the same time as completing this program. You've put up with my late nights and early mornings, always seeing me sitting at the table working on my computer. Thank you to you all. What a long strange trip it's been.

Table of Contents

List of Tables

List of Figures

Chapter One: Introduction

Climate Change in the Arctic

Arctic regions are complex, vast and offer important habitat for many mammals, fish and avian species, in addition to providing critical environment for the survival of Indigenous people. However, many Arctic areas have been dynamically changing due to increasing surface air temperatures, which have been amplified in northern regions as a result of climate change. Some of the greatest warming has been observed in the Arctic and sub-arctic, with certain areas experiencing increases in surface air temperatures of up to 2°C during the past several decades (Figure 1) (Chapin *et al*., 2005; Kaufman *et al*., 2009). Kaufman et al. (2009) reconstructed temperatures for the past 2000 years for regions poleward of 60°N and noted that four of the five warmest decades occurred between 1950 and 2000. Additionally, surface air temperatures in the Arctic are projected to rise another ~2.5°C by the mid-21st century and up to 5°C – 7°C by the end of the 21st century (ACIA, 2004).

Many northern landscapes are dominated by shallow freshwater lakes and ponds that provide important habitat for wildlife and waterfowl. Due to their small water volume and relatively large surface area, they are particularly susceptible to hydrological change. Evidence suggests some

Arctic lakes and ponds have already passed ecological thresholds as a result of warming (Smol and Douglas, 2007, 2008; Prowse *et al*., 2009). Many of these freshwater systems depend on snowmelt to sustain lake-water balances (Bowling *et al*., 2003). However, changes in snowfall and snowmelt, rainfall, permafrost thaw, as well as reduced duration of ice-cover and greater open-water evaporation, have the potential to strongly alter lake-water balances (Rouse *et al*., 1997; Schindler and Smol, 2006; Smol and Douglas, 2007).

Changes in northern landscapes due to climate variability are ongoing (Rowland *et al*., 2010) and direct observational data in polar regions are often lacking and sparse. This is especially true in northern areas where climate change has been amplified and warming is occurring at a faster rate than other areas on Earth (ACIA, 2004; Smol and Douglas 2007). Understanding how climate change is impacting the unique environment of the North is difficult due to the complexity and remoteness of the landscape. Thus, it is critical to implement long-term monitoring programs to provide knowledge of ecosystem health and trends and to help anticipate future changes.

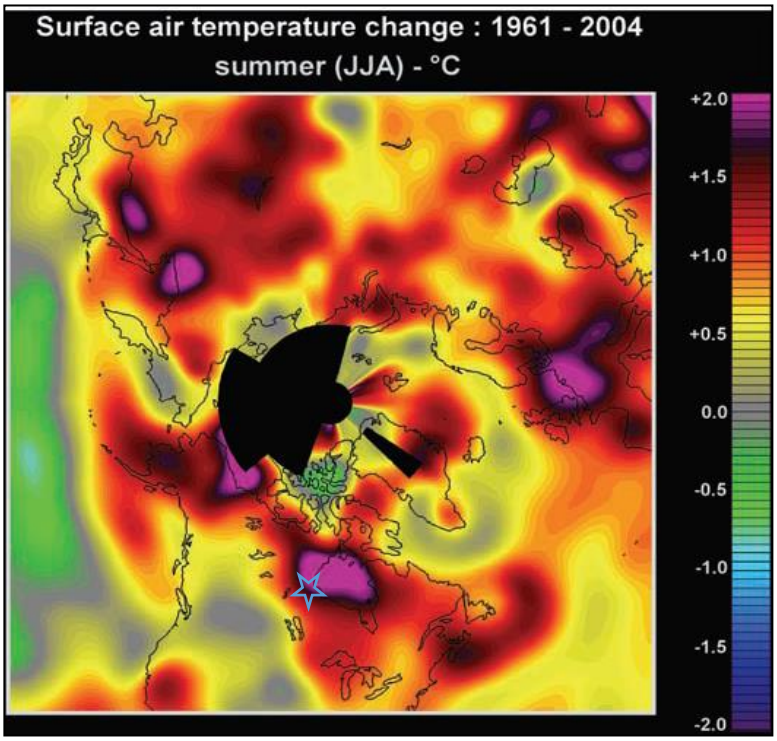

Figure 1. Average surface air temperature increases for June, July and August between 1961 and 2004 in Arctic and subarctic regions (Chapin *et al*. 2005; p 657). Hudson Bay and the Churchill region have experienced some of the greatest warming during the past ~50 years (denoted by a star). Purple areas represent surface air temperature increases up to 2°C on average.

Long-Term Aquatic Ecosystem Monitoring and Research Gaps

Due to climate change and changing northern landscapes, it is important to understand the ecological integrity of these areas. Ecological integrity refers to the natural condition of an ecosystem that is unaffected from human activity (Freedman *et al.,* 1995; Turner, 2005) and in which native components of the ecosystem have remained intact (Parks Canada,

2013). Ecological monitoring requires measuring and observing an ecosystem at regular intervals over an extended period of time to establish environmental baseline conditions of a region. This is useful for understanding changes that are observed outside the boundary of the natural baseline variability, and can provide reliable information to decision-makers for maintaining a healthy environment (Vaughan *et al.,* 2001). However, ecosystem health and integrity can be difficult to measure (Turner, 2005), especially in immense Arctic regions where numerous ecological factors act coincidentally. As a result, it can be challenging to implement monitoring plans that capture the diversity of a region.

Additionally, environmental issues have increased in complexity during the past few decades, generally since the start of the industrial revolution (~1800) which has led to a need to understand how different anthropogenic factors have had negative impacts on the environment. Studies on environmental changes due to climate warming in northern regions have been conducted across Canada since the early 20th century, however, substantial gaps exist in terms of long-term hydrological monitoring of Arctic ecosystems (Karlsson *et al.,* 2001). There have been numerous studies that involve data collection, yet few programs have implemented long-term monitoring with specific objectives (Mezquida *et al.,*

2005). Beever and Woodard (2010) have stated that integrating knowledge of different driving factors of ecosystems and long-term monitoring into ecosystem management is necessary.

Long-term water quality monitoring sites across Canada has been established by Environment Canada through federal and federal-provincial management since the 1980s. Aquatic monitoring of two major projects in Ontario and British Columbia, initiated in the late 1980s, has led to the Canadian Aquatic Biomonitoring Network (CABIN), which began in 2006 (Environment Canada, 2015). Although a positive step towards long-term water quality monitoring, CABIN has only been used for the past 10 years and there is still a lack of sampling and monitoring in many communities and regions throughout northern Canada (Environment Canada, 2015). Environment Canada has coordinated a partnership with the Ecological Monitoring and Assessment Network (EMAN), which was established in 1994, has 142 partners across Canada, and over 100 long-term environmental case study sites (Vaughan *et al.,* 2001). The mission of EMAN is to determine why ecosystem health is changing, and what can be done to implement long-term monitoring to better understand current and future conditions (Vaughan *et al.,* 2001). These partnerships have implemented

sampling and have monitored changes in water quality, however gaps still exist in understanding changes in water quantity.

In addition to these government monitoring projects, scientific research has been conducted in remote northern regions for the purpose of determining how environmental stressors are affecting hydrology of shallow lakes and ponds in permafrost terrain. For example, a study in Siberia using aerial imagery from the past 30 years shows significant decline in lake surface area from lake drainage, which was attributed to thawing permafrost from increasing air and soil temperatures (Smith *et al*., 2005). Riordan et al. (2006) and Carroll et al. (2011) have documented hydrological changes in regions of Alaska and Canada, respectively, using remote sensing, which have shown decreases in the size and abundance of lakes and ponds. Similarly, Beck et al. (2015) used remote sensing imagery in northern Quebec to conclude that between 2004 and 2009, 24 percent of lake surface area disappeared as a result of permafrost degradation. Moreover, as some areas have experienced a decreasing abundance of freshwater ecosystems, others have noted an increase in water surface area as well as the formation of new thermokarst lakes due to permafrost thaw and temperature increases (Jorgenson *et al*., 2013, Coulombe *et al*., 2016).

Conventional hydrological monitoring with sampling that occurs on a daily to weekly basis is difficult to implement in large remote regions due to the high cost of sampling, short field seasons and the instrumentation required (Keatley *et al*., 2006; Rowland *et al*., 2010). Additionally it is difficult to assess the hydrological implications of climate change on specific remote locations. However, it is crucial to implement long-term monitoring programs to better understand and observe changes and trends.

Hydrological Changes in Shallow Lakes and Ponds of the Hudson Bay Lowlands and Wapusk National Park

The geographic focus of this research is Wapusk National Park (WNP), northern Manitoba, located within the western Hudson Bay Lowlands (HBL). Shallow lakes and ponds (hereafter referred to as ponds for this study due to depth), many of which are thermokarst in origin, are a prominent landscape feature within WNP as they cover >50 percent of the park surface area. These ponds provide critical habitat for a variety of wildlife, including denning locations for polar bears. Due to seasonal ice cover of Hudson Bay, this region is typically colder than other areas at similar latitudes (Rouse, 1991). This ice cover generally lasts from late October to early June and has contributed to the presence of permafrost in the HBL as a result of extended periods of very cold temperatures (Markham, 1986; Gough and Leung, 2002).

Rising temperatures during the past half century have led to a reduction in sea ice cover and longer ice-free seasons over Hudson Bay (Parkinson *et al.,* 1999; Macrae *et al.,* 2014). Consequently, the timing and seasonal amounts of precipitation are expected to change (Gagnon and Gough, 2005), as warming is expected to increase the ice-free season over adjacent land areas (Sannel and Kuhry, 2011; Macrae *et al.,* 2014). Additionally, it has been observed that annual rainfall, based on measurements at the Churchill airport between 1943 and 2008, have increased by approximately 50 percent with the greatest increase in rainfall occurring in the late summer and early fall (Macrae *et al.*, 2014). With the rise in air and surface water temperatures, in addition to a longer ice-free season, increases in evaporation have been predicted (Rouse *et al*., 1997; Macrae *et al*., 2014).

Research during the past decade in WNP and surrounding areas indicate that the hydrology of shallow lakes and ponds are changing in response to shifting climate conditions (Wolfe *et al.,* 2011a; Bouchard *et al.,* 2013; Macrae *et al.,* 2014). In July 2004, Bos and Pellatt (2012) studied 32 ponds within and adjacent to WNP and determined that ponds are an expression of surface waters and had little connection to groundwater due to permafrost. A recent study indicated that observed lake desiccation in

northern Manitoba, attributed to a decline in snowmelt runoff, may be unprecedented during the past ~200 years (Bouchard *et al*., 2013). Additionally, Wolfe *et al.* (2011a) used cellulose-inferred pond water oxygen isotope records from sediment cores retrieved from ponds near Churchill, Manitoba, to determine that divergent changes in water balances are likely due to varied responses of hydrological connectivity as a result of 20th century warming. Furthermore, a recent study has shown increases in surface air temperatures and longer ice-free seasons with predicted increase in summer precipitation (Macrae *et al.,* 2014). Due to ongoing climate change, it is critical to implement long-term monitoring programs that allow for better understanding of the present and future implications that climate change will have on pond hydrology.

Water Isotope Tracers for Hydrological Monitoring

Due to the fact that many northern wetlands are difficult to access and that the cost of sampling is high in terms of time and resources, water isotope tracers have been increasingly used as they allow for surveying hydrological processes at a single point in time and can be applied to ongoing monitoring (Brock *et al*., 2007; Light, 2011; Tondu *et al.,* 2013; Turner *et al*., 2014). Previous studies have utilized water isotope tracers of oxygen and

hydrogen (^{18}O and ^{2}H) to characterize both the spatial and temporal variability of lake water balances (Gibson and Edwards., 2002; Wolfe *et al*., 2007; Tondu *et al*., 2013; Turner *et al*., 2014). A study by Gibson *et al.* (1993) used the stable isotope-mass balance method to estimate evaporation in two catchments in northern Canada as it is a useful metric to measure water balance. Brock *et al.* (2007) utilized water isotope tracers to characterize hydrology of shallow floodplain lakes in the Slave River Delta. Use of water isotope tracers for pond-water-balance-analysis allows for quantitative hydrological information to be obtained. Water isotope compositions are an excellent indicator of the hydrological processes that influence pond water balances, and are ideal to measure changes in the hydrological processes that influence ponds in WNP. As water isotope tracers can specify snowmelt, rainfall, and evaporation on pond water balance, they are ideal for studying ponds in remote locations such as WNP. Although studies have indicated change in hydrological conditions, there is still a lack of knowledge on the long-term influence that climate change will have on pond water balance. Thus, the need for determining current baseline conditions within the Park and understanding seasonal fluctuations on pond water balances. Knowledge of current conditions is necessary in order to recognise the range of natural

variability throughout the landscape. Water isotope sampling is straightforward, which makes it well-suited for agency-based monitoring.

A particularly relevant example of the use of water isotope tracers is a study by Tondu et al. (2013), which focuses on lakes in the Old Crow Flats (OCF) and Vuntut National Park (VNP), Yukon Territory. Similar to WNP, OCF-VNP is a northern, remote thermokarst landscape that contains many shallow lakes where there are concerns about the effects of climate change (Wolfe *et al.*, 2011b). An isotope framework was developed using an evaporation pan and applied for subsequent analysis of water isotope tracers (Tondu *et al.*, 2013). Tondu *et al.* (2013) utilized the coupled-isotope tracer method (Yi *et al*., 2008) to calculate input water isotope composition (δ_I) and evaporation-to-inflow (E/I) ratios. Using these water-balance metrics, supported by Turner et al. (2010, 2014), Tondu *et al.* (2013) established the foundation of a long-term hydroecological monitoring program. The 2016 field season marked the 10th consecutive year of sampling of lakes in OCF-VNP for water isotope analysis, which has been led by Parks Canada personnel for the past five years. This is the long-term vision for water isotope monitoring of ponds in WNP.

Long-Term Monitoring in Wapusk National Park

Wapusk National Park was established in 1996, and has many stakeholders involved in maintaining the ecological integrity of the park. The management board for the Park consists of the Government of Canada, the Government of Manitoba, the Town of Churchill, the Fox Lake Cree First Nation, and the York Factory First Nation (Parks Canada, 2013). Management for WNP agrees on the philosophy that the people are the 'Keepers of the Land' (Parks Canada, 2013). To maintain the collaborations between these groups, the first State of the Park Report (SoPR) was distributed in 2011 and offers the opportunity for the park management board to examine the challenges and successes of decisions made through the WNP management plan.

WNP is expected to provide a new SoPR every 10 years, with the next Park Management Plan to be published along with the Wapusk National Park Ecological Integrity Monitoring Plan (WNPEIMP) for 2015-2025. The current SoPR report (2011) for the freshwater indicator on aquatic ecosystems is not yet rated (SoPR, 2011, pg. 3). Therefore, this research will contribute to a hydrological monitoring program that is in the process of being implemented for WNP by Parks Canada. The monitoring program for hydrology within the

park will be a result of previous sampling and studies (Wolfe *et al*., 2007; Farquharson, 2013; White, PhD in progress) in addition to results presented in this thesis. It is anticipated that results from six years of isotope-based hydrological monitoring will be integrated into the Park Management Plan within the SoPR. The WNPEIMP will also include information pertaining to monitoring for wetlands, permafrost, snowpack, bear denning, coastal ecosystems and effects of Snow Goose populations. Currently, Wapusk National Park is working with researchers from Wilfrid Laurier University and the University of Waterloo to create standard operating procedures (SOP) that will be incorporated into the hydrological monitoring protocols for sampling ponds within the park (White *et al.*, 2016).

Research Objectives

This research aims to understand the present-day hydrological conditions of a representative suite of ponds in the three main ecozones (boreal spruce, peat-plateau palsa-bog, and coastal fen) of Wapusk National Park. One of the objectives of Parks Canada is to "provide clean and scientifically-defensible assessments of the ongoing ecological integrity condition of national parks" (Parks Canada, 2007, pg. 2). As efforts increase to incorporate more monitoring and environmental knowledge into park

management, long-term monitoring holds the key for assessing the ongoing ecological integrity of WNP. Results from this thesis will be shared with Parks Canada to assist with their objective to provide assessments of ecological integrity within WNP. This will be done by developing an isotope framework that can be implemented into a long-term hydrological monitoring program for tracking pond hydrology in the Park.

The specific research objectives include:

(1) Evaluate different approaches for developing an 'isotope framework' to be utilized for current and ongoing long-term hydrological monitoring of ponds in WNP.

(2) Use water isotope tracers measured on a representative suite of ponds in WNP from 2010-2015 and apply an isotope-mass balance model to calculate input water isotope composition (δ_I) and evaporation to inflow (E/I) ratios to characterize the relative roles of snowmelt, rainfall and evaporation on pond water balances and their spatial, seasonal and annual variability, as well as their relations with catchment and meteorological conditions.

Expected outcomes of this research include the development and implementation of methods that have long-term viability and sustainability

to ensure that Parks Canada will be able to continue monitoring into the future. By applying coupled analysis of water isotope measurements on ponds for hydrological monitoring in WNP, impacts that environmental stressors have on the ponds may be observed through trends and changes in pond water balances over time. Ongoing monitoring of lake water isotope compositions and determination of δ_I and E/I values will provide key metrics for identifying changes in lake-water balances as applied by Tondu *et al*. (2013).

Chapter Two: Study Area and Methods

Study Area

The Hudson Bay Lowlands (HBL) are located along Hudson Bay in the northern region of Ontario and Manitoba and a small northwestern portion of Quebec. The HBL is the largest wetland in North America and is mainly characterized by bogs and coastal fen with water covering >50% of the surface area (Parks Canada, 2010). The HBL was under the Laurentian Ice Sheet as recently as 9,000 years ago with the thickest ice cover occurring over Hudson Bay (Stella *et al*., 2007). Due to the landscape being depressed from the glaciation, it is now in a state of isostatic rebound with a rise of approximately one meter per century (Webber *et al*., 1970; Johnson *et al*., 1987). The underlying geology is Silurian and Ordovician sedimentary rocks as well as monzonite, granodiorite and charnockite that overlies Precambrian sandstone, limestone and dolomite (Sanford *et al.* 1968; Dredge and Nixon, 1992). Due to fine-grained marine sediment and glacial till, the region has developed into an extensive wetland, with flat muskeg areas of peatlands, low-drainage areas and thermokarst lakes (Dredge and Nixon, 1992).

Wapusk National Park (WNP) (57^{o}N, 97^{o}W) was founded in 1996 to protect 11,475 km^{2} of sub-arctic habitat that spans a region of continuous

and discontinuous permafrost along the western shores of Hudson Bay in Manitoba (Figure 2a, b) (Parks Canada, 2015). The average depth of permafrost ranges between 30-60 m with ground temperatures of approximately -2°C (Rouse *et al*., 1997). Due to permafrost, impermeable substrate, and isostatic rebound, the WNP landscape consists of freshwater topographic and thermokarst water bodies that cover up to ~50 % of the total area (Parks Canada, 2015). There are three prominent ecozones in WNP that are characterized by dominant vegetation: coastal fen, interior peat plateau-palsa bog (hereafter referred to as peat plateau), and boreal spruce (Parks Canada, 2012). The coastal fen is distinguished by salt marshes and dunes, with up to 10 foot tides along the coastal beaches (Parks Canada, 2012). The peat plateau is marked by tundra vegetation consisting of sedge meadows, peatlands and ponds (Parks Canada, 2012). The boreal spruce forest consists of spruce, tamarack and willows of the northern taiga forest and is located in the southwestern region of the Park (Parks Canada, 2012). Ponds in the boreal spruce ecozone tend to be the largest and deepest.

Ponds Chosen for Hydrological Monitoring

Sixteen ponds were selected for isotope-based hydrological monitoring from an original 37-pond data set sampled between 2010 and

2012 (Farquharson, 2013). The ponds were chosen to cover the range of hydrological conditions across the Park's three main ecozones (Figure 3). Most of the ponds are typically less than 1 m in depth with those in the boreal spruce ecozone being less than 3 m in depth. They likely freeze completely during winter months and are ice-free during summer months (3 - 4 months of the year). Most ponds contain bottoms that consist of a benthic mat, with a few ponds hosting macrophytes. The topography of the area is very flat and gently sloping towards Hudson Bay (1 m km^{-1}) (Winter and Woo, 1990). Most ponds are disconnected from surrounding peatlands and do not have defined outlet channels. As a result, ponds in this study are considered closed-drainage. Ponds WAP 5, 7, 12, 15, 20 and 21 are located in the coastal fen ecozone, and range between 2.4 km and 16.7 km in distance from the Hudson Bay coast (Table 1). The coastal fen ponds range in size from 700 m^2 to 23,059 m^2 (WAP 12 is not reported due to low resolution satellite imagery), but are all less than ~3 m in depth. Vegetation in the surrounding catchments of coastal fen ponds consist of small willows, grasses, lichens and mosses. Ponds WAP 32, 33, 34, 37 and 39 are located in the peat plateau, located farther inland between 41.7 km and 52.8 km from Hudson Bay (Table 1). The area of these ponds ranges from 132 m^2 to 7,613,782 m^2, and all are less than 60 cm in depth. However WAP 39 may be

up to 2 m in depth (field observations have determined pond waters to be deeper than 60 cm although actual depths have not been measured from a central pond location). These ponds have catchments that consist of grasses, small shrubs and willows that range in size up to 1 m tall. Ponds WAP 23, 24, 25, 26 and 27 are located in the boreal spruce forest and are located farthest from Hudson Bay, between 82.4 km to 89.9 km (Table 1). They range in size from 98,000 m^2 to 2,686,414 m^2 in area and range between ~1 m to 3 m in depth.

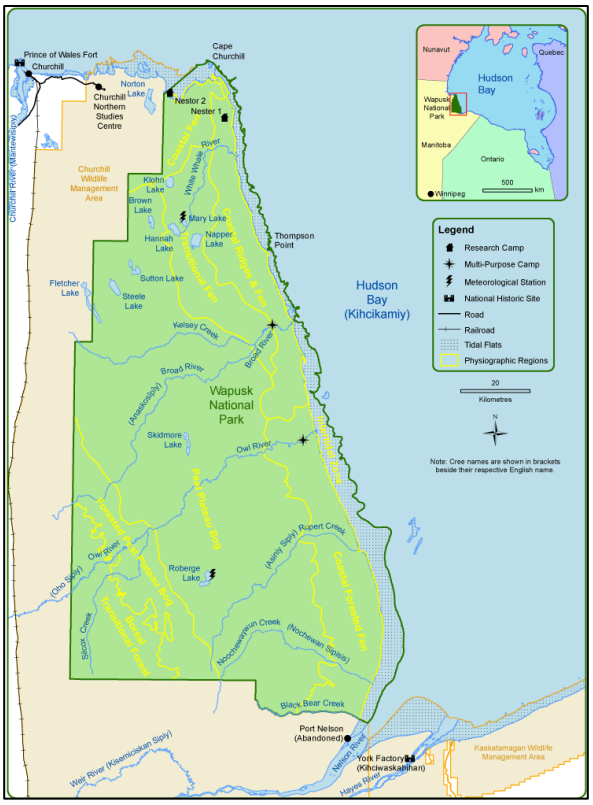

Figure 2a) Location of Wapusk National Park, Manitoba (Parks Canada, 2016).

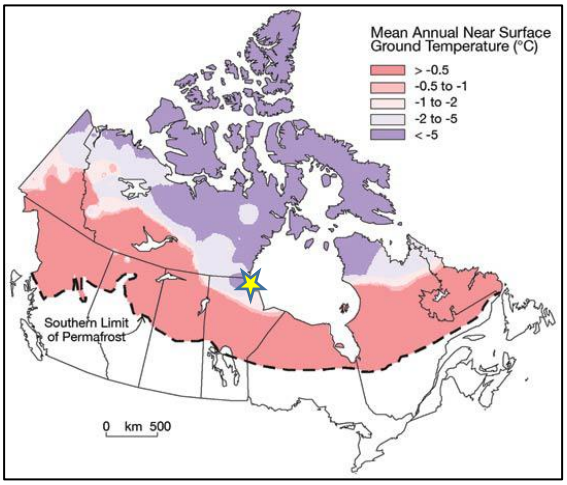

Figure 2b) Wapusk National Park (denoted by a star) is located in an area of continuous and discontinuous permafrost (NRCAN, 2016).

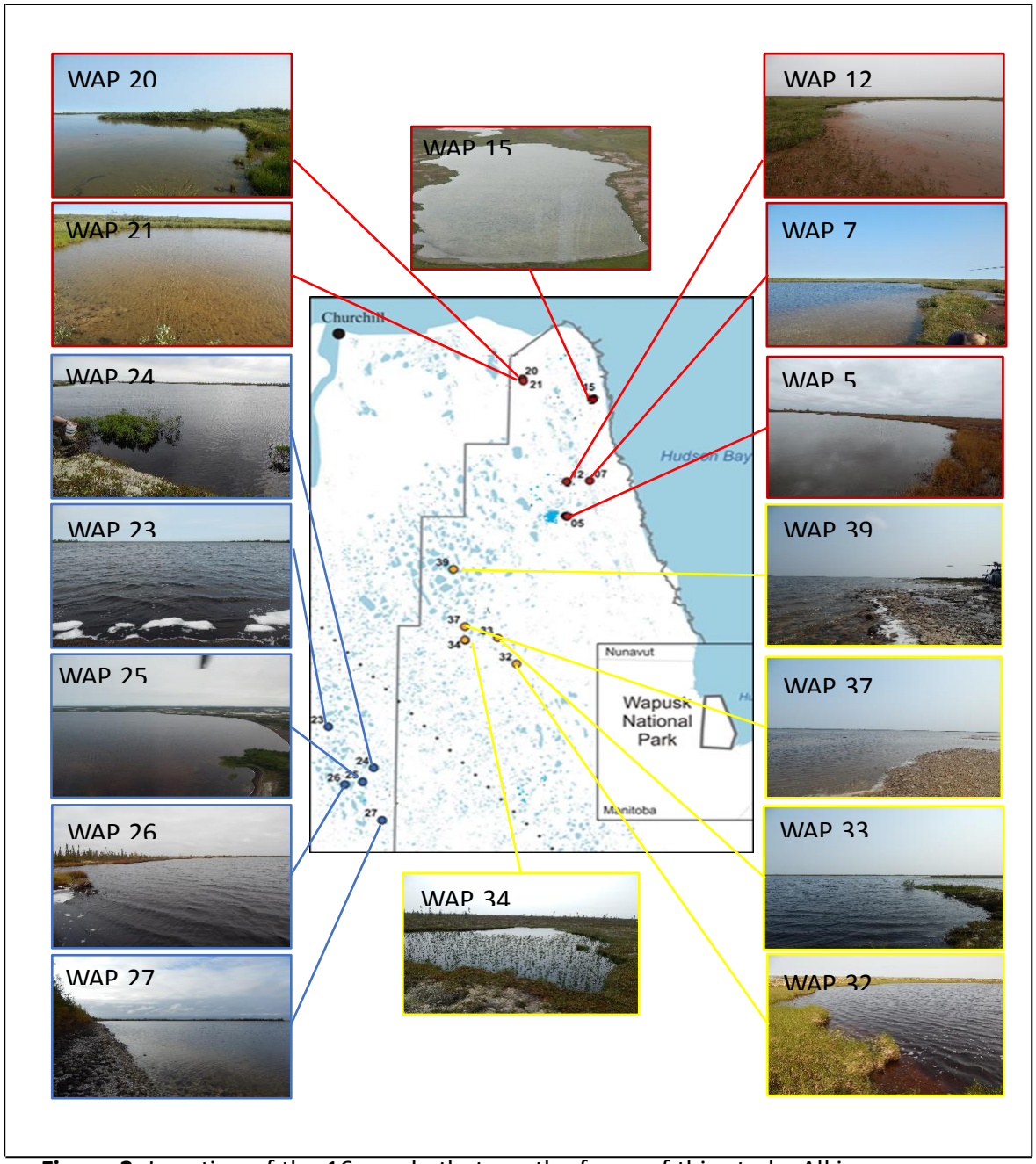

Figure 3. Location of the 16 ponds that are the focus of this study. All images were captured in July 2014 except photos for WAP 5, 26 and 27, which were taken in September 2014. Red outline denotes ponds in coastal fen ecozone, yellow outline denotes ponds in the Interior peat plateau ecozone and blue outline represent ponds in the boreal spruce ecozone.

Table 1. List of 16 ponds selected for isotope-based hydrological monitoring for effects of climate change. Distance from Hudson Bay and pond surface area calculated by Farquharson (2013). WAP 12 area is not reported due to low-resolution satellite imagery. Pond depth is an average value and is estimated based on multiple field season observations.

Pond Name	Ecozone	Pond Depth (cm)	Area (m^2)	Latitude	Longitude	Distance from Hudson Bay (km)
WAP05	Coastal Fen	5-10	2,290	58.34223	-93.2645	13.81
WAP07	Coastal Fen	5-30	25,843	58.42721	-93.1782	9.07
WAP12	Coastal Fen	<1	NA	58.42558	-93.2689	14.74
WAP15	Coastal Fen	15	93,724	58.62001	-93.1710	2.47
WAP20	Coastal Fen	5	23,059	58.66995	-93.4437	14.42
WAP21	Coastal Fen	5-10	700	58.66515	-93.4409	16.70
WAP32	Interior Peat Plateau	60	531	57.99007	-93.4593	41.79
WAP33	Interior Peat Plateau	60	12,605	58.05161	-93.5329	44.88
WAP34	Interior Peat Plateau	5	132	58.04637	-93.6592	52.87
WAP37	Interior Peat Plateau	<10	1,366,129	58.07802	-93.6610	50.83
WAP39	Interior Peat Plateau	15- >200	7,613,782	58.21463	-93.7076	47.73
WAP23	Boreal Spruce	15- >200	1,087,513	57.83547	-94.1827	89.17
WAP24	Boreal Spruce	15- >200	98,200	57.73882	-94.0051	82.46
WAP25	Boreal Spruce	15- >200	2,686,414	57.70476	-94.0465	86.33
WAP26	Boreal Spruce	15- >200	177,365	57.69803	-94.1149	89.96
WAP27	Boreal Spruce	15- >200	1,196,026	57.61421	-93.9695	88.39

Meteorological Conditions

The climate in WNP is seasonal with short, warm summers and long, cold winters. Pond freeze-up in WNP typically occurs mid- to late September and ice-breakup occurs between late May and mid-June. Meteorological conditions were classified into two seasons for the purpose of this study (ice-on: October to May and ice-free: June to September). Climate normal air temperature (1981-2010), as recorded at the Churchill Airport (Climate ID 5060600), is -6.5°C with temperatures fluctuating between -30.1°C in January to 26.7°C in July (Environment Canada, 2015) (Figure 4). Average annual precipitation (1981-2010 climate normal) is 452.7 mm, with 53.7% falling as rain (243.3 mm) from June to September. This study incorporates water isotope compositions from ponds collected during the 2010-2015 ice-free seasons. Therefore, it is relevant to consider meteorological conditions during this interval as temperature, humidity and precipitation will influence the isotope compositions of the ponds. If average monthly and seasonal temperatures were one degree warmer or cooler or more than climate normal, they are highlighted with red or blue (Table 2). Total monthly and seasonal precipitation are reported as wetter (blue) or drier (red) than climate normal (Table 3).

Overall, there is annual variability in meteorological data.

Meteorological data for the six sampling years shows mean monthly air temperatures for the ice-free season are higher than the 1981- 2010 climate normal for 2011 to 2014 (Table 2, Figure 4). Average temperature values for ice-on season are relatively similar to the climate normal for all sampling years with only 2012 having a warmer average value (Table 2). Total ice-free rainfall is less than the climate normal for all study years except for 2010. However, data over the six-years show much less than climate normal rainfall during early ice-free season with an increase in rainfall amounts during the mid-ice-free season (July and August). Additionally, winter snowfall was below climate normal (1981 – 2010) for all sampling years (Table 3). Data over the six-years suggests that the region was experiencing warmer conditions than the climate normal with drier winters and drier ice-free total rain amounts.

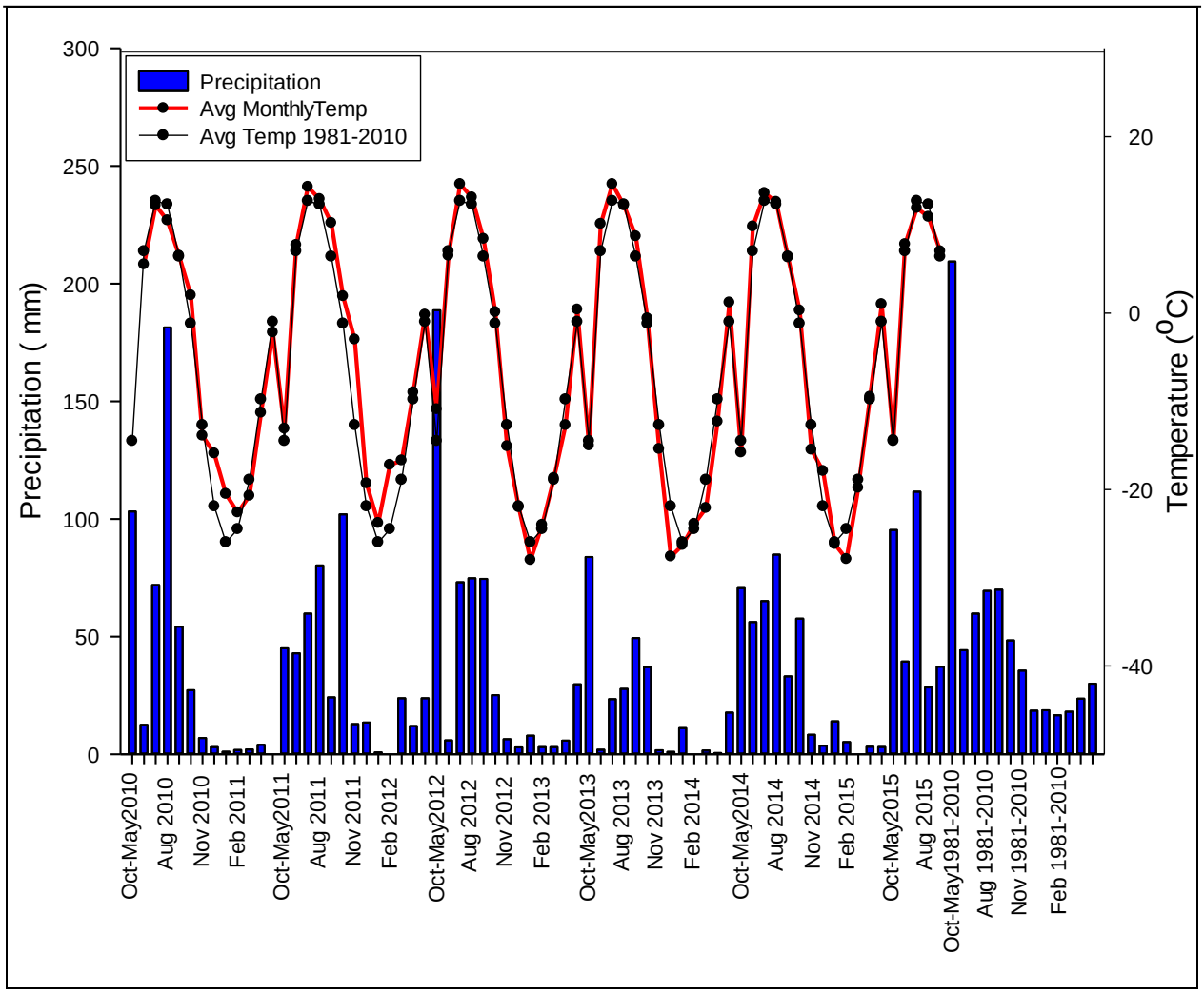

Figure 4. Average monthly and seasonal temperature and precipitation as recorded by Environment Canada (2015) Churchill meteorological station (Climate ID 5060600) for October 2009 to September 2015. Climate normal (1981-2010) monthly and seasonal temperature are also shown.

Table 2. Average monthly and seasonal temperatures in degrees Celsius as recorded by Churchill Airport (Climate ID 5060600) station, Environment Canada (2015). Red numbers indicate values that are one degree warmer or more than the 1981-2010 average, while values in blue represent those one degree cooler or more than the average. Average values reported for Oct-May indicate average monthly temperatures from the previous year (e.g., Oct-May 2010 represents average monthly temperature from Oct 2009-May 2010).

Month	1981-2010	2010	2011	2012	2013	2014	2015
June	7.0	5.5	7.7	6.5	10.1	9.8	7.8
July	12.7	12.2	14.3	14.6	14.6	13.6	11.9
August	12.3	10.5	12.9	13.1	12.2	12.6	10.9
Sept	6.4	6.5	10.2	8.4	8.7	6.3	7.0
Avg. Ice-Free	9.6	8.6	11.2	10.6	11.4	10.5	9.4
Oct-May	-14.5	-14.2	-13.1	-10.9	-15.0	-15.8	-14.4

Table 3. Total monthly and seasonal precipitation (mm) as recorded by Churchill Airport (Climate ID 5060600) station, Environment Canada (2015). Red numbers indicate values that are lower (drier) than the 1981-2010 average, while values in blue represent those higher (wetter) than the average. Average values reported for Oct-May indicate average monthly precipitation from the previous year (e.g., Oct-May 2010 represents average monthly precipitation from Oct 2009-May 2010).

Month	1981-2010	2010	2011	2012	2013	2014	2015
June	44.2	12.5	42.9	5.9	1.9	56.2	39.4
July	59.8	71.9	59.8	73.1	23.4	65.1	111.6
August	69.4	181.4	80.2	74.8	27.8	84.8	28.4
Sept	69.9	54.2	24.2	74.5	49.4	33.1	37.2
Ice-Free total	243.3	320.0	207.1	228.3	102.5	239.2	216.6
Oct-May	209.4	105.8	46.0	188.7	83.8	70.6	95.6

Methods

Field Methods

The 16-pond dataset was sampled after ice-off, mid-summer and before ice-on (June, July and September) between 2010 and 2015 with the aid of a helicopter. A hand-held GPS, in addition to pond photographs, were used to ensure that samples were collected from the same pond each time.

Samples were collected from 5 to 10 cm below the surface water of ponds using 30 mL high density polyethylene bottles. Once water samples were collected, the bottles were sealed tightly and transported to the University of Waterloo Environmental Isotope Laboratory (UW-EIL) for analysis of oxygen and hydrogen isotope compositions.

A constant volume evaporation pan was deployed at the Wapusk National Park main office in Churchill, MB, and was monitored by Parks Canada staff during June to September of 2010-2015. The evaporation pan was used to simulate a terminal basin (i.e., closed-drainage) at isotopic and hydrologic steady-state where inflow is equal to evaporation (δ_{SSL}). The source of water input for the evaporation pan was derived from the Churchill River and the pan was maintained at a constant water level with samples collected weekly during each ice-free season for analysis of oxygen and hydrogen isotope composition**.**

Laboratory Methods

Water samples were transported to UW-EIL where they were analysed for hydrogen and oxygen isotope compositions. Samples submitted between 2010 and 2012 were analysed with continuous flow isotope ratio mass spectrometry using standard methods (Epstein and Mayeda, 1953; Coleman et al. 1982). Maximum analytical uncertainties for $\delta^{18}O$ and $\delta^{2}H$ are

± 0.2 ‰ and ± 2.0 ‰, respectively, for samples analysed by mass spectrometry. Samples from 2013 and onward were analysed using Off-Axis Integrated-Cavity Output Spectroscopy (ICOS). This method has maximum analytical uncertainties of ± 0.1 ‰ for $\delta^{18}O$ and ± 0.3 ‰ for $\delta^{2}H$. Both methods are reported relative to Vienna Standard Mean Ocean Water (VSMOW) and results are normalized to -55.5‰ and -428‰, respectively, for Standard Light Antarctic Precipitation (Coplen, 1996). The delta (δ) notation is used to express the isotope composition values in units per mil (‰) with respect to VSMOW, where $\delta^{2}H$ or $\delta^{18}O = [(R_{sample} / R_{standard}) - 1] \times 1000$ where R is the $^{18}O/^{16}O$ and $^{2}H/^{1}H$ ratios in both the sample and standard.

Water Isotope Mass-Balance Modelling

As water passes through the hydrological cycle, labelling of naturally occurring stable isotopes of hydrogen (^{1}H and ^{2}H) and oxygen (^{16}O, ^{17}O and ^{18}O) occurs due to the differences in behaviours of water molecules (Clark and Fritz, 1997). These isotope compositions are expressed through the differences in abundances between the rare (heavy) isotope species and the common (light) isotope species. Due to systematic mass-dependent fractionation of isotope compositions of precipitation and surface water, patterns exist characterized by linear trends in $\delta^{2}H$ - $\delta^{18}O$ space (Gibson and Edwards, 2002; Edwards *et al*., 2004). Isotopic compositions of precipitation

typically cluster along the Global Meteoric Water Line (GMWL; $\delta^2H = 8\delta^{18}O + 10$), as defined by Craig (1961) for worldwide amount-weighted annual precipitation. The slope of eight is generally influenced by temperature-dependent equilibrium fractionation of the formation of precipitation from atmospheric vapour (Edwards *et al*., 2004). At regional scales, precipitation can plot in a linear trend on a Local Meteoric Water Line (LMWL; Dansgaard, 1964; Gibson *et al.,* 1993). The LMWL is often similar to the GMWL but requires isotopic measurements on local precipitation to define. However, if unavailable, the GMWL often provides a useful baseline of precipitation isotope composition (Edwards *et al.,* 2004). Based on Rayleigh distillation and isotope rain-out effects, snow is typically more isotopically depleted in comparison to rain (Clark and Fritz, 1997).

In a region experiencing the same climatic conditions, surface waters that have undergone varying degrees of evaporation will typically plot along a Local Evaporation Line (LEL), which commonly has a slope of ~4-6 (Figure 5). The slope is controlled by humidity (*h*), temperature (T) and the isotope composition of atmospheric moisture (δ_{AS}) (Yi *et al*., 2008), and can be predicted for a given location (e.g., Wolfe *et al.,* 2007). The LEL can be calculated using the linear resistance model of Craig and Gordon (1965) and

by incorporating local isotopic and hydroclimatic information. Calculating the LEL, as opposed to the more common approach of using linear regression through water samples that have undergone varying degrees of evaporation, allows for lake water isotope compositions to be interpreted independent of, but in relation to, the LEL. The position of a water body along and about the LEL can indicate importance of evaporation and source waters, respectively. Water bodies that plot above the LEL typically reflect influence by rainfall, whereas water bodies that fall below the LEL generally indicate influence from snowmelt. Three key points on the LEL include 1) the amount-weighted mean annual precipitation (δ_p at the GMWL-LEL intersection), 2) the limiting steady-state isotope composition (δ_{SSL}), and 3) the theoretical limiting isotopic enrichment (δ^*) of a pond reaching total desiccation. The isotope compositions of all ponds within a similar region will converge towards δ^* as a body of water reaching desiccation is dependent on atmospheric conditions (temperature and relative humidity) and is independent of initial conditions (i.e., δ_L, δ_I) (Yi *et al.,* 2008).

Developing the Local Evaporation Line

Multiple approaches were used to evaluate and establish the 'isotope framework' (i.e., GMWL-LEL) as it was critical to define for subsequent

calculation of water-balance metrics (δ_I, E/I) and in consideration of ongoing Parks-led hydrological monitoring. The different iterations of the LEL were all anchored at δ_p. This value was determined from www.waterisotopes.org, which provides monthly values of precipitation isotope composition for any location based on latitude, longitude, and elevation (Bowen, 2016).

Two different frameworks were used to determine δ_{SSL}. The first approach used the equation that defines δ_{SSL} provided by Gonfiantini (1986; note that all equations are reported in decimal notation):

$$\delta_{SSL} = \alpha^*\delta_I(1-h+\varepsilon_K) + \alpha^* h\delta_{AS} + \alpha^*\varepsilon_K + \varepsilon^* \quad (1)$$

where α^* is the equilibrium liquid-vapour fractionation factor, δ_I is assumed to be equal to δ_P, *h* is the atmospheric relative humidity, δ_{AS} is the isotope composition of atmospheric moisture during the ice-free season, whereas ε^* and ε_K represent the equilibrium and kinetic isotope separation between liquid and vapour, respectively.

For α^*, the equation by Horita and Wesolowski (1994) was used:

$$1000 ln\alpha^* = -7.685 + 6.7123\ (10^3/T) - 1.6664\ (10^6/T^2) + 0.35041\ (10^9/T^3) \quad (2)$$

for $\delta^{18}O$ and

$$1000 ln\alpha^* = 1158.8\ (T^3/10^9) - 1620.1\ (T^2/10^6) + 794.84\ (T/10^3) - 161.04 + 2.9992\ (10^9/T^3) \quad (3)$$

for δ^2H where temperature (T) is in Kelvin.

Kinetic separation (ε_K) was calculated using Gonfiantini (1986) where:

$$\varepsilon_K = 0.0142\ (1\text{-}h) \text{ for } \delta^{18}O \quad (4)$$

and

$$\varepsilon_K = 0.0125\ (1\text{-}h) \text{ for } \delta^2H. \quad (5)$$

The equilibrium isotope separation between the liquid and vapour phase (ε^*) was determined from:

$$\varepsilon^* = (\alpha^* - 1) \quad (6)$$

The value for δ_{AS} was determined by (Gibson *et al.,* 2008):

$$\delta_{AS} = (\delta_{PS} - \varepsilon^*)/\alpha^* \quad (7)$$

which assumes isotopic equilibrium with the isotope composition of open-water season precipitation (δ_{PS}). The value for δ_{PS} was obtained from www.waterisotopes.org (June to September).

To determine the terminus of the LEL, the limiting isotope composition of a water body approaching desiccation (δ^*) was determined using Gonfiantini (1986):

$$\delta^* = (h\delta_{AS} + \varepsilon_K + \varepsilon^*/\alpha^*) / (h - \varepsilon_K - \varepsilon^*/\alpha^*) \quad (8)$$

The second framework determined δ_{SSL} using results from the evaporation pan experiment. For each year, δ_{SSL} was calculated from the average of values estimated to have reached steady-state conditions. For the LEL that utilized δ_{SSL} from the evaporation pan experiment, δ_{AS} was determined using Gibson *et al.* (1999):

$$\delta_{AS} = [(\delta_{SSL} - \varepsilon^*) / \alpha^* - \varepsilon_K - \delta_P (1 - h + \varepsilon_K)] / h. \quad (9)$$

In equation (9), δ_{SSL} was determined from the evaporation pan.

Values for T and *h* were obtained from Environment Canada's National Climate Archive (Environment Canada, 2015). These data were flux-weighted based on estimates of potential evapotranspiration following Thornthwaite (1948):

$$T_{flux} = \Sigma (T_a * E_t)/(E_t) (^oC) \quad (10)$$

$$h_{flux} = \Sigma (h * E_t)/(E_t) (\%) \quad (11)$$

where T_a represents the monthly average temperature and *h* represents the monthly average humidity. The value of E_t represents monthly total potential evapotranspiration for ice-free season months given by the equation:

$$E_t = 1.6 * (L/4) * (N/30) * ((10*T_a)/I)^a \quad (cm) \qquad (12)$$

where L represents average day length in hours (Environment Canada, 2015). The value of N represents the number of days in the month and I is the thaw season heat index, which is calculated by:

$$I = \Sigma ((T_a{}^{1.534})/5) \quad (^oC) \qquad (13)$$

where the coefficient *a* is calculated by:

$$a = 0.49239 + 0.01792 * I - 7.7 * 10^{-5} * I^2 + 6.75 * 10^{-7} * I^3 \qquad (14)$$

Calculation of Water Balance Metrics

Results from isotope analysis of pond water samples were plotted in $\delta^{18}O$-$\delta^{2}H$ space to identify the hydrological influences on pond water balances (i.e., input sources and evaporation). Using the coupled isotope tracer approach (Yi *et al*., 2008), the isotope composition of input water (δ_I) was determined for each pond and for each sampling episode. Using this approach, the isotope composition of pond evaporative vapour (δ_E) was

determined using the linear resistance model of Craig and Gordon (1965), which is provided by Gonfiantini (1986) as:

$$\delta_E = [(\delta_L - \varepsilon^*)/ \alpha^* - h\delta_{AS} - \varepsilon_K]/ (1 - h + \varepsilon_K) \quad (15)$$

Using δ_E and δ_L, a pond-specific evaporation line was determined and the intersection with the GMWL was used to define δ_I (Figure 5). The value of δ_I was used to identify the predominant source water (i.e., snowmelt, rainfall) for the ponds. Then evaporation to inflow (E/I) ratios for each pond and for each sampling episode were determined by the equation from Yi et al. (2008):

$$E/I = (\delta_I - \delta_L)/(\delta_E - \delta_L) \quad (16)$$

where δ_L is the measured isotope composition of pond water.

E/I is a useful metric for lake hydrological monitoring as it can be used to quantify pond water balances (Gonfiantini, 1986; Gibson and Edwards, 2002; Wolfe et al., 2007; Turner et al., 2010; Light, 2011). These metrics (δ_I, E/I) have successfully been used to quantify lake water balances in the Slave River Delta (Brock *et al*., 2008) and the Old Crow Flats (Turner *et al*., 2010) and has been applied for a hydrological monitoring program in Vuntut National Park, Yukon Territory (Tondu *et al*. 2013). Calculated E/I values that

were above 1.5 were given a value of 1.5 as the framework could not be used to accurately calculate E/I ratios for ponds experiencing extreme non-steady-state conditions (Tondu *et al*., 2013; MacDonald *et al*., 2017).E/I values were analysed spatially, temporally and in relation to catchment characteristics (ecozone) and meteorological conditions to assess hydrological balances of ponds in WNP.

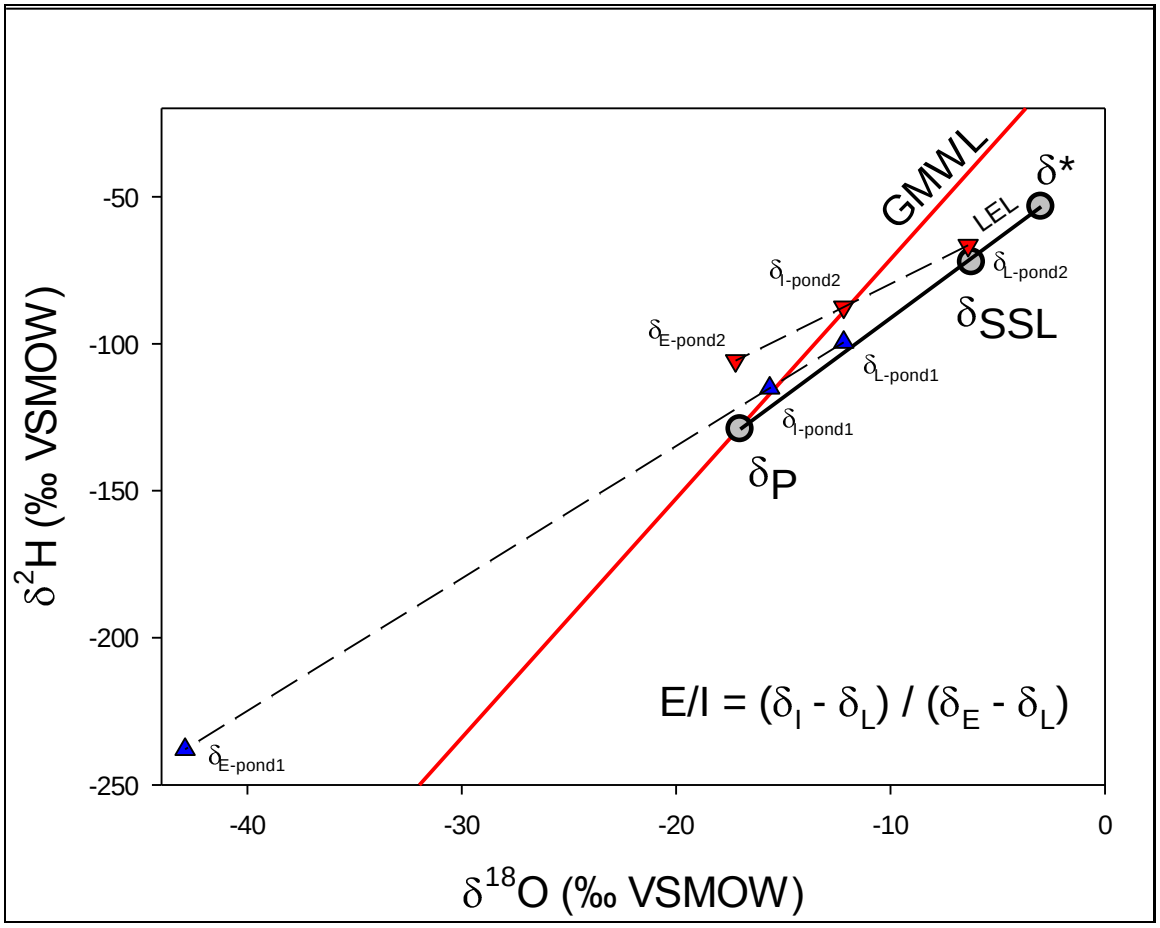

Figure 5. Schematic $\delta^{18}O$-$\delta^{2}H$ diagram representing two ponds from WNP (pond 1=coastal fen, pond 2=boreal spruce). Key parameters within this plot include: amount weighted mean annual precipitation (δ_P), the limiting steady-state isotope composition where evaporation is equal to inflow (δ_{SSL}), and limiting isotope enrichment of a pond reaching total desiccation (δ^*); all of which make up the Local Evaporation Line (LEL). Both ponds plot along a pond specific evaporation line which intersects with the Global Meteoric Water Line (GMWL). This intersection provides an estimate of input water (δ_I) which is used for isotope mass balance model calculations to derive evaporation-to-inflow (E/I) ratios. Other values used to calculate E/I include pond water isotope composition (δ_L) and the isotope composition of evaporated vapour from the pond (δ_E).

Chapter 3 - Results

Typically, the regional isotope composition of precipitation will cluster along a Local Meteoric Water Line (LMWL), which is often similar to the Global Meteoric Water Line (GMWL; Craig, 1961). Light (2011) calculated the Churchill LMWL using a linear regression model and Canadian Network for Isotopes in Precipitation data. Based on the similarity between the LMWL and the GMWL, Light (2011) determined that the GMWL suitably characterized the isotope composition of precipitation for the region. As surface waters of ponds experience evaporation, they plot below the GMWL forming a linear trend along the Local Evaporation Line (LEL). The amount of mass-dependent fractionation that pond water isotope composition experiences (i.e., water molecules containing the lighter isotopes will preferentially evaporate) will influence the distance a pond plots from the GMWL. Values that define the LEL include the average annual isotope composition of precipitation (δ_P), where the LEL intersects the GMWL, the steady-state isotope composition of a terminal basin (δ_{SSL}) and the theoretical last drop of water in a pond (δ^*). For the purpose of this study, two isotope frameworks were developed to assess their appropriateness for subsequent interpretation of the pond water isotope compositions and calculation of water balance metrics. One isotope framework was developed

using Gonfiantini's (1986) formulation for δ_{SSL} (see equation 1 in Chapter 2) and values were averaged over the 6-year period of the study (hereafter referred to as the *Gonfiantini Framework*). A second isotope framework was developed using an evaporation pan to determine δ_{SSL}, and then framework values were averaged over the 6-year period of the study (hereafter referred to as the *Pan Framework*).

Developing the *Gonfiantini Framework*

The *Gonfiantini Framework* was developed to assess its appropriateness for characterizing pond water isotope composition in WNP. Values derived are reported in Table 4. Flux weighted temperature and humidity were calculated from meteorological data collected at the Churchill Airport, which were obtained from Environment Canada (2015). The isotope composition of precipitation (δ_P) was obtained through www.waterisotopes.org. Values for δ_{SSL} and δ^* were calculated using equations 1 and 8, respectively (Chapter 2). Values for δ_{AS} were determined from equation 7. The slope of the LEL is based on the linear regression model of Craig and Gordon (1965) through δ_P, δ_{SSL} and δ^* (Table 4).

Table 4. Results of calculations to develop the *Gonfiantini Framework.*

Parameter	2010	2011	2012	2013	2014	2015	Mean	Stand. Dev.	Ref.
T (K)	282.4	284.7	284.4	284.9	284.3	282.9	283.4	1.02	Env. Canada (2015)
h (%)	80.39	77.31	77.69	73.13	74.87	81.79	77.53	3.25	Env. Canada (2015)
α^* (^{18}O, ^{2}H)	1.0108, 1.098	1.0106, 1.094	1.0107, 1.096	1.015, 1.094	1.0106, 1.095	1.0108, 1.097	1.0114, 1.095	0.0017, 0.001	2, 3 (equations, Ch. 2)
ε^* (^{18}O, ^{2}H)‰	10.8, 97.9	10.6, 94.9	10.6, 95.2	10.5, 94.5	10.6, 95.3	10.8, 97.3	10.6, 95.8	0.12, 1.39	6
ε_K(^{18}O, ^{2}H)‰	28.2, 25.0	32.2, 28.3	31.2, 27.5	38.0, 33.5	35.5, 31.2	25.9, 22.8	31.8, 27.8	4.4, 4.0	4,5
δ_{AS}(^{18}O, ^{2}H)‰	-24.2, -185.1	-24.1, -183.0	-24.1, -183.6	-24.0, -182.7	-24.1, -183.4	-24.2, -184.5	-24.1, -183.7	1.3, 6.1	7
δ_{SSL}(^{18}O, ^{2}H) ‰	-9.4, -90.5	-8.8, -88.8	-9.0, -89.4	-8.0, -86.1	-8.2, -86.6	-9.8, -91.9	-8.9, -88.9	0.6, 5.0	1
δ^* (^{18}O, ^{2}H)‰	-7.5, -79.5	-6.3, -75.1	-6.7, -76.6	-4.5, -67.8	-5.0, -69.4	-8.1, -82.4	-6.4, -75.2	0.5, 3.1	8
δ_P(^{18}O, ^{2}H) ‰	-17.0, -129.0	-17.0, -129.0	-17.0, -129.0	-17.0, -129.0	-17.0, -129.0	-17.0, -129.0	-17.0, -129.0		www.waterisotopes.org
Slope	5.4	5.3	4.9	5.3	5.3	5.1	5.2		
Intercept	-36.8	-38.2	-44.3	-38.4	-38.8	-41.0	-39.5		

All pond water isotope compositions were plotted for each sampling time on the six-year average LEL to evaluate suitability of the *Gonfiantini Framework* (Figure 6). Pond water isotope compositions plot past δ^* during 2010-2013 implying that ponds have desiccated (Figure 6). However, only two ponds in 2010 completely desiccated (WAP 10 and WAP 12) based on field observations (Farquharson, 2010). Also, nearly every pond water

isotope composition plots above the LEL indicating that the primary influence on pond water balance is rainfall, although some ponds are also very likely influenced by snowmelt. These results suggest that the *Gonfiantini Framework* may not provide the most suitable LEL for interpreting pond water isotope compositions.

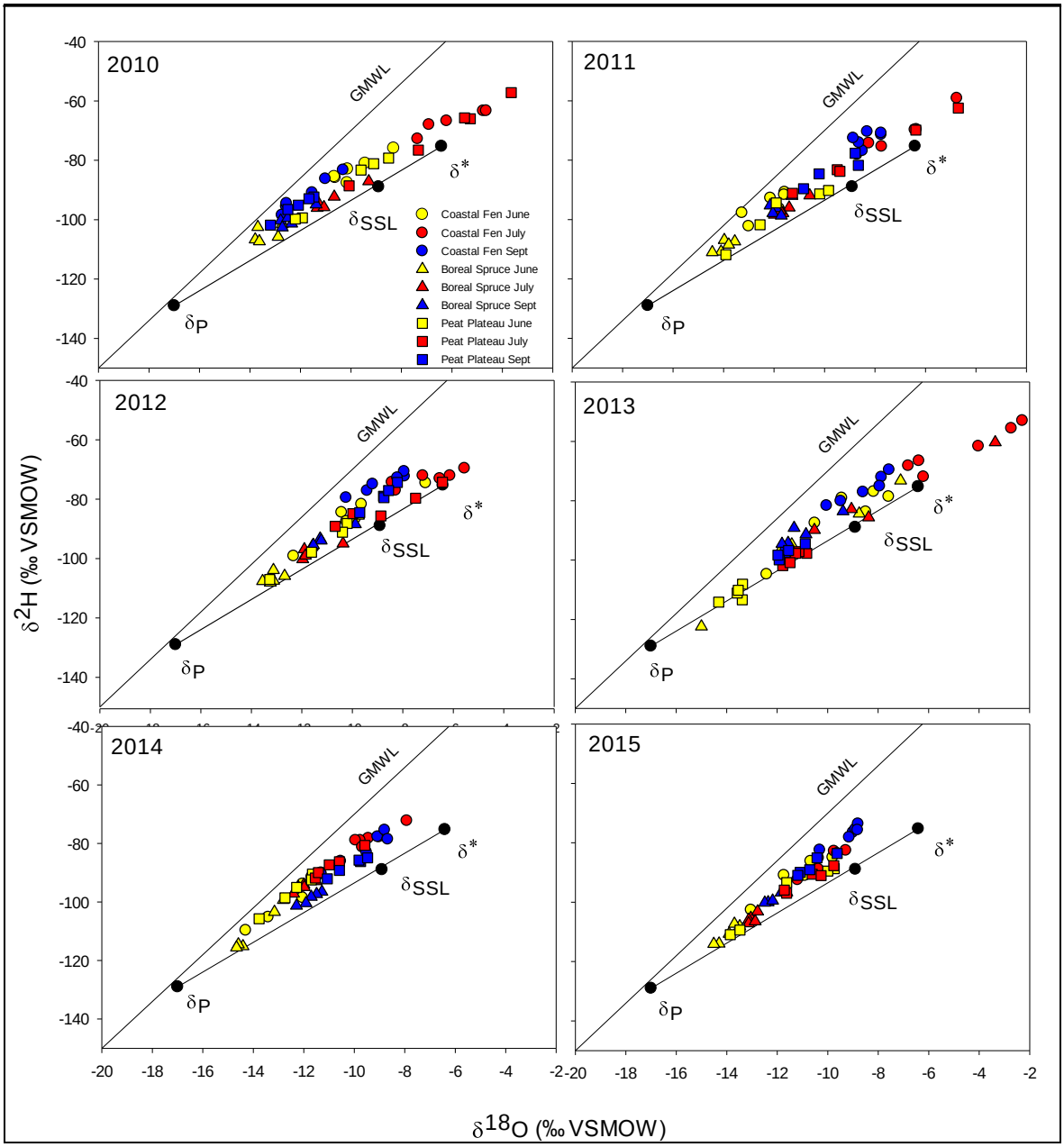

Figure 6. Pond water isotope compositions superimposed on the *Gonfiantini Framework.*

Developing the *Pan Framework*

The *Pan Framework* was developed to assess its appropriateness for interpreting pond water isotope compositions. Values derived are reported in Table 5. Similar to the *Gonfiantini Framework,* flux weighted temperature and humidity were calculated from 1981-2010 climate normals, which were obtained from Environment Canada (2015). Also, the isotope composition of precipitation (δ_P) was obtained through www.waterisotopes.org and values for δ^* were calculated using equation 8 (Chapter 2). In contrast to the *Gonfiantini Framework,* values for δ_{SSL} were based on evaporation pan data (see below and Figure 7), and this was then used to determine δ_{AS} using equation 9. All values were averaged to generate a six-year mean.

Table 5. Results of calculations to develop the *Pan Framework.*

Parameter	2010	2011	2012	2013	2014	2015	Mean	Stand. Dev.	Ref.
T (K)	282.4	284.7	284.4	284.9	284.3	282.9	283.4	1.02	Env. Canada (2015)
h (%)	80.39	77.31	77.69	73.13	74.87	81.79	77.53	3.25	Env. Canada (2015)
α^* (^{18}O, ^{2}H)	1.0108, 1.098	1.0106, 1.094	1.0107, 1.096	1.015, 1.094	1.0106, 1.095	1.0108, 1.097	1.0114, 1.095	0.0017, 0.001	2, 3 (equations, Ch. 2)
ε^* (^{18}O, ^{2}H)‰	10.8, 97.9	10.6, 94.9	10.6, 95.2	10.5, 94.5	10.6, 95.3	10.8, 97.3	10.6, 95.8	0.12, 1.39	6
ε_K(^{18}O, ^{2}H)‰	28.2, 24.0	32.2, 28.3	31.2, 27.5	38.0, 33.5	35.5, 31.2	25.9, 22.8	31.8, 27.8	4.4, 4.0	4,5
δ_{AS}(^{18}O, ^{2}H)‰	-19.3, -157.9	-19.9, -158.4	-20.2, -170.3	-22.3, -168.2	-22.3, -169.9	-19.7, -158.4	-20.6, -163.8	1.3, 6.1	9
δ_{SSL}(^{18}O, ^{2}H)‰	-5.5, -66.8	-5.6, -68.5	-6.0, -78.8	-6.8, -74.8	-7.1, -76.6	-6.1, -68.4	-6.2, -72.3	0.6, 5.0	1
δ^* (^{18}O, ^{2}H)‰	-2.6, -49.3	-2.2, -48.1	-3.0, -54.0	-2.9, -51.9	-3.7, -56.5	-3.6, -53.9	-3.0, -52.2	0.5, 3.1	8
δ_P(^{18}O, ^{2}H) ‰	-17.0, -129.0	-17.0, -129.0	-17.0, -129.0	-17.0, -129.0	-17.0, -129.0	-17.0, -129.0	-17.0, -129.0		www.waterisotopes.org
Slope	4.56	5.04	5.33	5.03	5.04	3.95	4.82		
Intercept	-41.58	-39.96	-40.42	-40.46	-40.66	-44.20	-41.21		

During all six sampling years, isotopic enrichment occurred during the first four weeks of deploying the evaporation pan (Figure 7a). This occurred as pan water isotope composition equilibrated with atmospheric conditions. The interval in which $\delta^{18}O$ became near-constant (i.e., reached steady state) was different each year and the mean values for these intervals were used to determine $\delta^{18}O_{SSL}$ (and $\delta^{2}H_{SSL}$) (14 July to 11 Aug 2010: $\delta^{18}O_{SSL}$ = -5.5 ‰,

δ^2H_{SSL} = -66.8 ‰; 5 July to 16 Aug 2011: $\delta^{18}O_{SSL}$ = -5.6 ‰, δ^2H_{SSL} = -68.5 ‰; 11 July to 9 Aug 2012: $\delta^{18}O_{SSL}$ = -6.0 ‰, δ^2H_{SSL} = -78.8 ‰; 5 July to 23 Aug 2013: $\delta^{18}O_{SSL}$ = -6.8 ‰, δ^2H_{SSL} = -74.7 ‰; 3 July to 28 Aug 2014: $\delta^{18}O_{SSL}$ = -7.1 ‰, δ^2H_{SSL} = -76.6 ‰; 17 July to 11 Sept 2015: $\delta^{18}O_{SSL}$ = -6.1 ‰, δ^2H_{SSL} = -68.4 ‰). These data were used to determine six-year mean $\delta^{18}O_{SSL}$ (-6.2 ± 0.6 ‰) and δ^2H_{SSL} (-72.3 ± 5.0 ‰; Table 5, Figure 7c). Evaporation pan isotope composition clusters along the LEL indicating influence from precipitation and evaporation (Figure 7b). During some portions of August and September, the evaporation pan was influenced by isotopically-depleted rainfall and, therefore, these data were not used to determine δ_{SSL}.

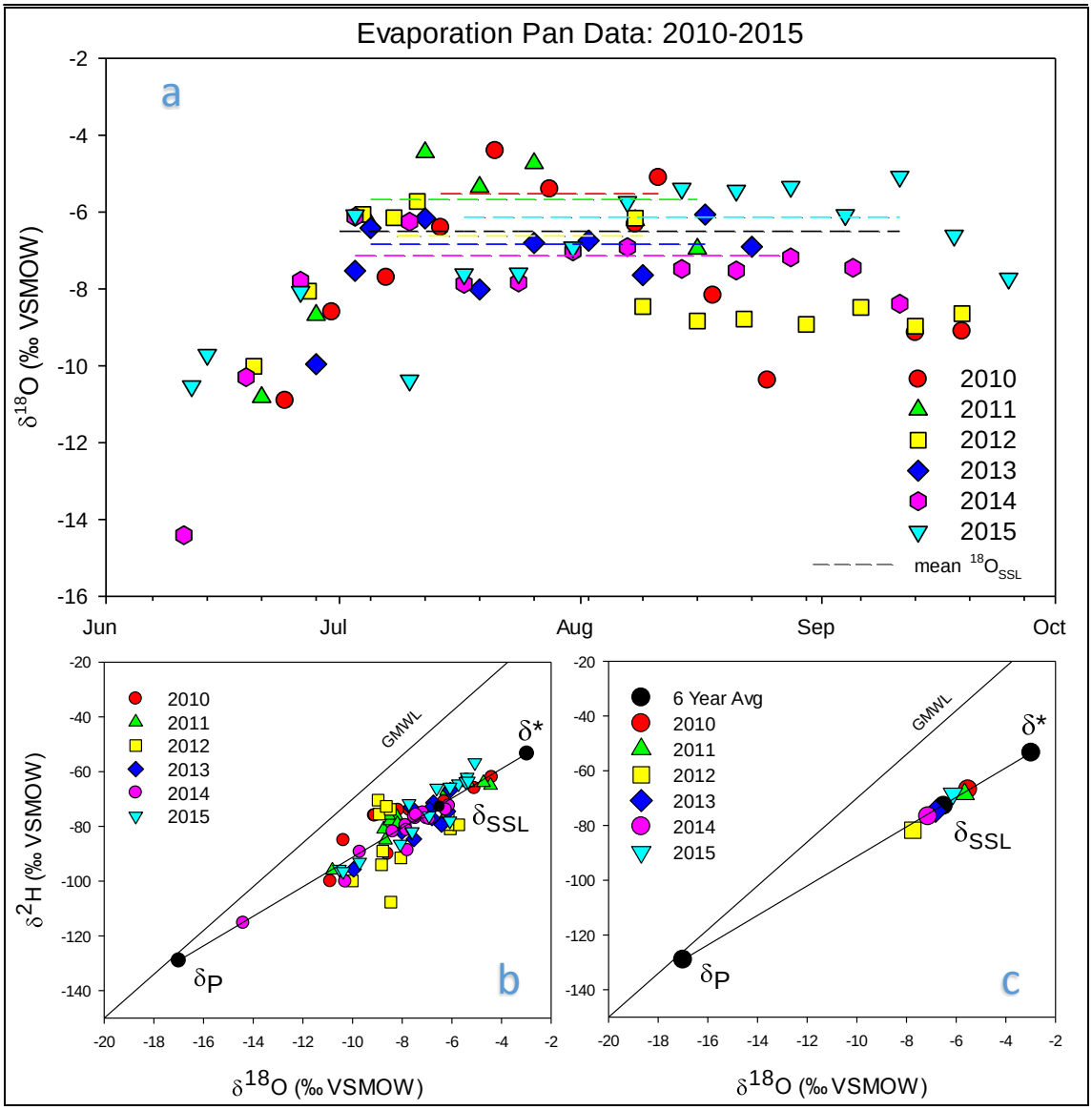

Figure 7. Isotope results from the evaporation pan deployed and maintained at the Wapusk National Park main office in Churchill, MB. A) Evaporation pan water oxygen isotope composition. Dashed lines represent intervals interpreted to represent steady state conditions (i.e., δ_{SSL}). B) Water isotope composition clusters on and around the LEL. C) Yearly and six-year average δ_{SSL} values.

Pond water isotope compositions were superimposed on the *Pan Framework* to evaluate its appropriateness for interpreting the pond water isotope compositions (Figure 8). The pond water isotope compositions are well captured by the parameters of the *Pan Framework* for all of the sampling years (aside from three ponds; WAP 5, WAP 12 and WAP 26 in 2013 which plot beyond δ^*). In particular, most evaporatively-enriched ponds during 2010-2013 do not exceed δ^*, indicating that these ponds were undergoing water-level drawdown but did not fully desiccate, which is consistent with field observations. In addition, while most pond water isotope compositions plot above the LEL, several plot on the LEL. Based on these features, the *Pan Framework* was determined to be appropriate for interpreting pond water isotope compositions.

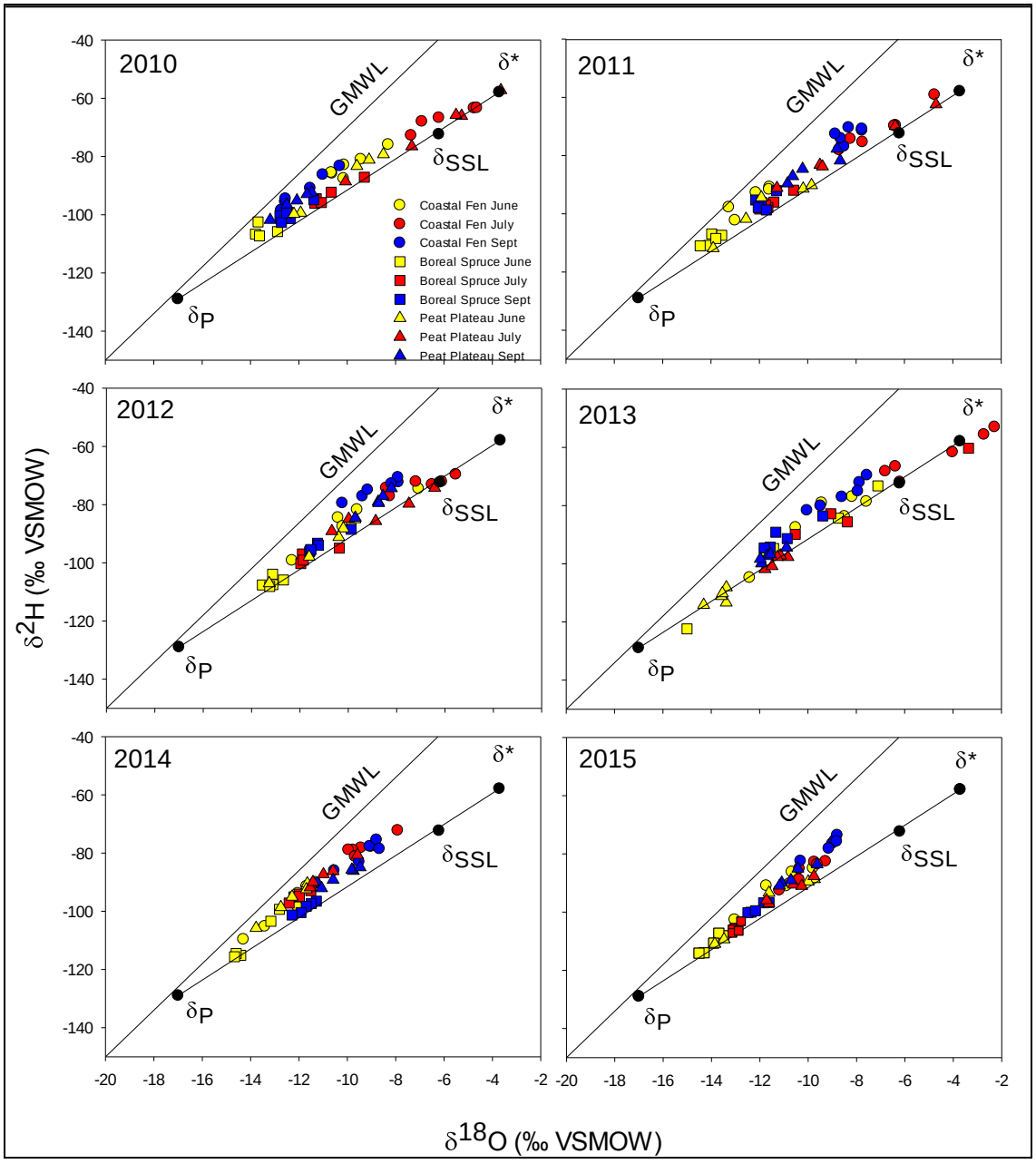

Figure 8. Pond water isotope compositions superimposed on the *Pan Framework.*

Pond Water Isotope Composition

Although there is a broad range of variability in pond water isotope composition during the six years of sampling ($\delta^{18}O_L$ = -15.0‰ to -0.86‰ and $\delta^{2}H_L$ = -122.3‰ to -51.6‰), there are distinct temporal and spatial patterns (Figure 8). Annual variability is evident with the greatest range in pond water isotope composition in 2013 (WAP 26: $\delta^{18}O_L$ = -15.0‰, $\delta^{2}H_L$ = -122.3‰ to WAP 25: $\delta^{18}O_L$ = -3.3‰, $\delta^{2}H_L$ = -60.3‰). In contrast, the smallest range in pond water isotope composition occurred in 2015 (WAP 26: $\delta^{18}O_L$ = -14.5‰, $\delta^{2}H_L$ = -114.0‰ to WAP 15: $\delta^{18}O_L$ = -8.7‰, $\delta^{2}H_L$ = -73.5‰).

Variability exists among the six years, however pond water isotope compositions show generally similar patterns in seasonal isotopic evolution (Figure 8). Pond water isotope compositions are generally lower on the LEL during the early ice-free season (June) due to the influence of isotopically-depleted snowmelt and possibly rainfall. Pond water isotope compositions then become more isotopically enriched during the mid-ice-free season (July) due to evaporation and plot higher on the LEL, around and beyond δ_{SSL} (Figure 8). During the later ice-free season (September), pond water isotope compositions plot lower on the LEL and are generally more isotopically depleted compared to July because of the influence of rainfall. These pond

water isotope composition changes indicate a wet-dry-wet pattern over the course of the ice-free season. Pond water isotope compositions show the most seasonal variability between 2010 and 2013. Pond water values become more enriched during July, with some ponds plotting past δ_{SSL} and towards and beyond δ^* during 2013 (WAP 5: $\delta^{18}O$= -2.7‰, δ^2H = -55.5‰; WAP 12: $\delta^{18}O$= -2.2‰, δ^2H = -52.9‰; WAP 25: $\delta^{18}O$= -3.3‰, δ^2H = -60.3‰) (Figure 8). In contrast, all pond water isotope compositions plot below δ_{SSL} during 2014-2015 and occupy a smaller range in $\delta^{18}O - \delta^2H$ space compared to the previous four years. Although there is variability in pond water isotope compositions, regardless of season, year or ecozone, most ponds plot above the LEL. This indicates that rainfall is an important source of the water in ponds as values that plot above the LEL indicate influence from rainfall.

In addition to seasonal variability, distinct patterns exist between the three ecozones. Coastal fen ponds show the greatest range in $\delta^{18}O - \delta^2H$ space during all six sampling years with the greatest range in 2013 (WAP 20: $\delta^{18}O_L$ = -12.0‰, δ^2H_L = -104.7‰ to WAP 5: $\delta^{18}O_L$ = -2.2‰, δ^2H_L = -52.9‰) (Figure 8). Water isotope composition of ponds in the coastal fen ecozone typically plot on or above the LEL with only five ponds plotting below the LEL (July 2012: WAP 5, WAP 12; July 2013: WAP 5, WAP 12, WAP 21) (Figure 8).

Ponds in the coastal fen ecozone show the greatest influence from summer evaporation of all ecozones, and this is most distinct from 2010 and 2013. During these years, many coastal fen ponds plot near and beyond δ_{SSL} during the mid-ice-free season.

Water isotope compositions of ponds in the peat plateau ecozone show variability with the greatest range in $\delta^{18}O - \delta^{2}H$ space during 2010 (WAP 32: $\delta^{18}O_L$ = -13.1‰, $\delta^{2}H_L$ = -101.8‰ to WAP 32: $\delta^{18}O_L$ = -3.6‰, $\delta^{2}H_L$ = -57.2‰) and 2011 (WAP 37: $\delta^{18}O_L$ = -13.9‰, $\delta^{2}H_L$ = -111.8‰ to WAP 32: $\delta^{18}O_L$ = -4.6‰, $\delta^{2}H_L$ = -62.4‰) (Figure 8). Ponds in the peat plateau ecozone display similarities to ponds in the coastal fen ecozone between 2010 and 2012 as they plot lower on the LEL during early ice-free season. Ponds then plot around and past δ_{SSL} during the mid-ice-free season and become depleted again during the later ice-free season (Figure 8). During 2013-2015, however, ponds in the peat plateau ecozone show more similarities in seasonal evolution to those in the boreal spruce ecozone.

Pond water isotope composition of boreal spruce ponds typically show the smallest range in $\delta^{18}O - \delta^{2}H$ space among ecozones during all years except 2013 (Figure 8). These ponds plot closer to δ_P than ponds in the coastal fen and peat plateau ecozones during most sampling times, indicating

that they are the ponds most influenced by precipitation and least influenced by evaporation. During mid-ice-free season, boreal spruce ponds plot closer to δ_{SSL}, however, only in 2013 do boreal spruce ponds exhibit a large range in $\delta^{18}O - \delta^{2}H$ space and one pond plots past δ_{SSL} (WAP 24: $\delta^{18}O_L$ = -3.3‰, $\delta^{2}H_L$ = -60.3‰) (Figure 8). Boreal spruce pond water isotope compositions during 2013 exhibit similarities to pond water isotope values in the coastal fen ecozone.

Isotope Composition of Input Water

Calculations of pond-specific input water isotope compositions (δ_I) were used to characterize the nature of source water to ponds in WNP. δ_I values were estimated by the intersection of the pond-specific LELs and the GMWL (Yi *et al.*, 2008). Pond source waters were defined by δ_I relative to δ_P, such that $\delta_I \leq \delta_P$ indicates predominantly snowmelt whereas $\delta_I > \delta_P$ indicates predominantly rainfall (Turner *et al.*, 2010). Note, however, δ_I values for WAP 5, 12, 21 and 25 could not be calculated during July 2013 as the framework fails to accurately capture these values because pond water isotope composition plot beyond δ^* (Figure 8). Distribution of pond water δ_I values along the GMWL was used to assess variation in source waters among ponds in the three ecozones (Figure 9). δ_I values during the six-year period display

variability between ecozones. Ponds within the peat plateau and boreal spruce ecozones have average δ_I values, which tend to be slightly higher than δ_P indicating preferential influence by rainfall. Ponds in the coastal fen ecozone appear to be more rainfall-dominated as their δ_I values plot higher on the GMWL.

Although, there does not appear to be any long term trends towards increasing or decreasing $\delta^{18}O_I$ values over the six years, seasonal variability in $\delta^{18}O_I$ values is evident for many of the ponds (Figure 10). $\delta^{18}O_I$ is generally low during early ice-free season (June). There is typically an increase in $\delta^{18}O_I$ values during mid-ice-free season (July) with a decline during the late ice-free season (September). This may indicate a) the decrease in supply of snowmelt and b) increase in influence of rainfall during the ice-free season. Some ponds exhibit $\delta^{18}O_I$ values that fall below δ_P during June and July (WAP 5, 12, 20 and 21) (Figure 10) indicating possible influence from early ice-free season snowmelt during these times. Additionally, some ponds display an increase in δ_I values in both July and September during 2010-2012 (Figure 10) indicating rainfall is a contributing factor to pond water balance.

Spatial patterns of $\delta^{18}O_I$ values are apparent among ecozones (Table 6). Coastal fen and peat plateau ponds possess a similar amount of variability

in $\delta^{18}O_I$ values whereas boreal spruce ponds have the smallest amount of variability (Table 6). Generally, ponds in the coastal fen had the highest average $\delta^{18}O_I$ values (-13.5‰), followed by peat plateau ponds (-15.1‰) and then boreal spruce ponds (-15.6‰) (Table 6; Figure 10). These values indicate that pond water balance in the coastal fen is most influenced by rainfall, followed by ponds in the peat plateau and boreal spruce forest. Ponds in the coastal fen ecozone display the greatest amount of variability in $\delta^{18}O_I$ values compared to the other two ecozones, with the exception of WAP 7 which displays low variability in $\delta^{18}O_I$ values (Figure 10). Indeed, WAP 7 has the smallest range in $\delta^{18}O_I$ values of all ponds (WAP 7: $\delta^{18}O_I$ = -13.6‰ to -11.7‰; standard deviation = 0.56; Table 6).

Among ponds in the peat plateau ecozone, WAP 32 displays the greatest amount of variability in $\delta^{18}O_I$ values ($\delta^{18}O_I$ = -19.2‰ to -12.4‰; standard deviation = 2.08; Table 6) (Figure 10). In contrast, WAP 33 has the smallest range in $\delta^{18}O_I$ values ($\delta^{18}O_I$ = -16.8‰ to -13.2‰; standard deviation = 1.14; Table 6). All ponds in the peat plateau possess $\delta^{18}O_I$ values that fall below δ_P during June and July of some years, indicating influence from snowmelt (Figure 10).

Ponds in the boreal spruce ecozone show the least variability of $\delta^{18}O_I$ values over the six years (Table 6, Figure 10). However, WAP 23 displays the greatest amount of variability in $\delta^{18}O_I$ values ($\delta^{18}O_I$ = -17.8‰ to -6.0‰; standard deviation = 2.56; Table 6) (Figure 10). In contrast, WAP 24 has the smallest range in $\delta^{18}O_I$ values ($\delta^{18}O_I$ = -16.9‰ to -14.1‰; standard deviation = 0.76; Table 6). Boreal spruce pond $\delta^{18}O_I$ values plot closest to δ_P and all ponds have sample times that plot below δ_P indicating that their pond water balances are more influenced by snowmelt than ponds from the other ecozones (Figure 10).

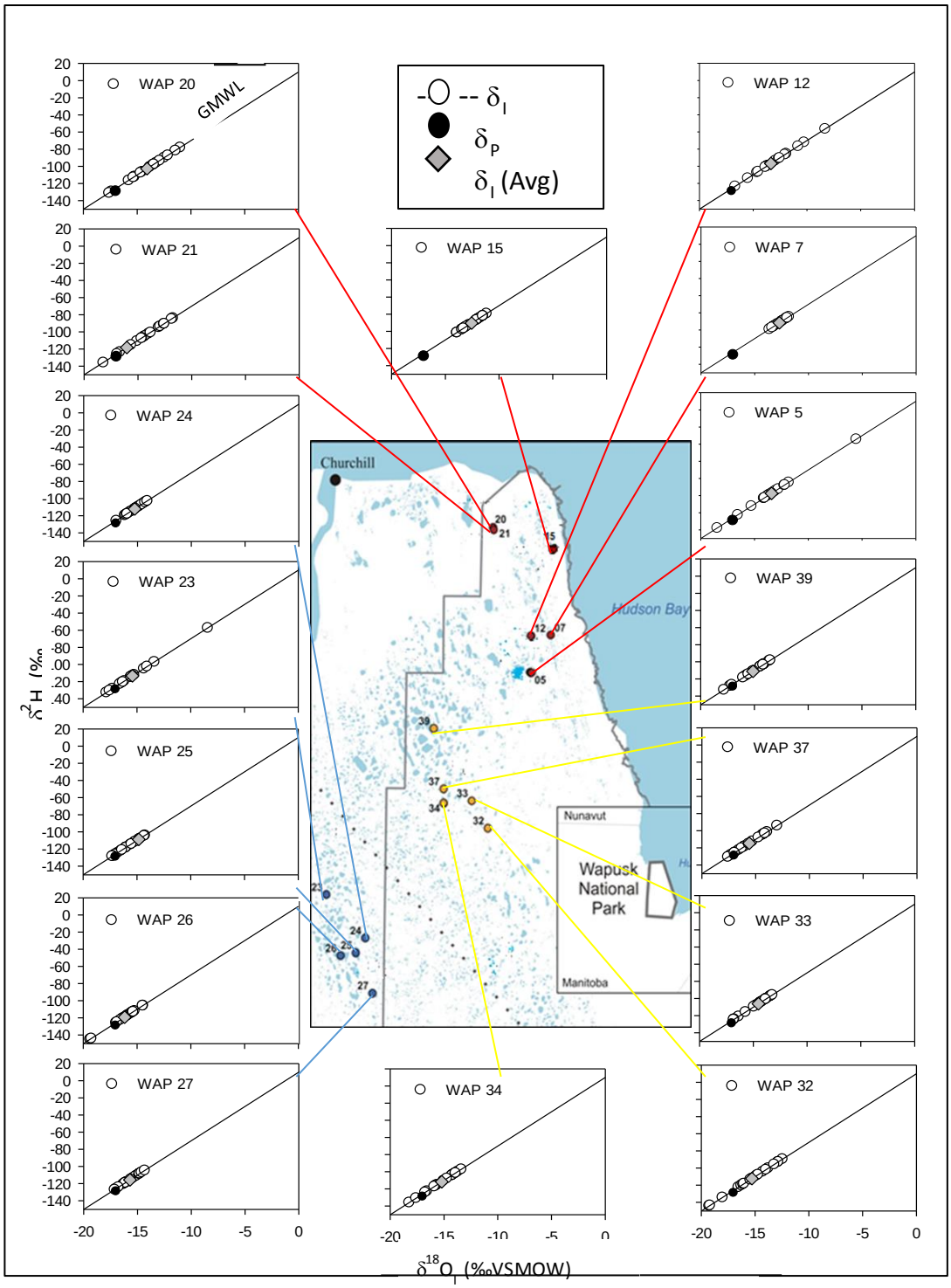

Figure 9. Calculated input water isotope composition (δ) for each pond from 2010 to 2015.

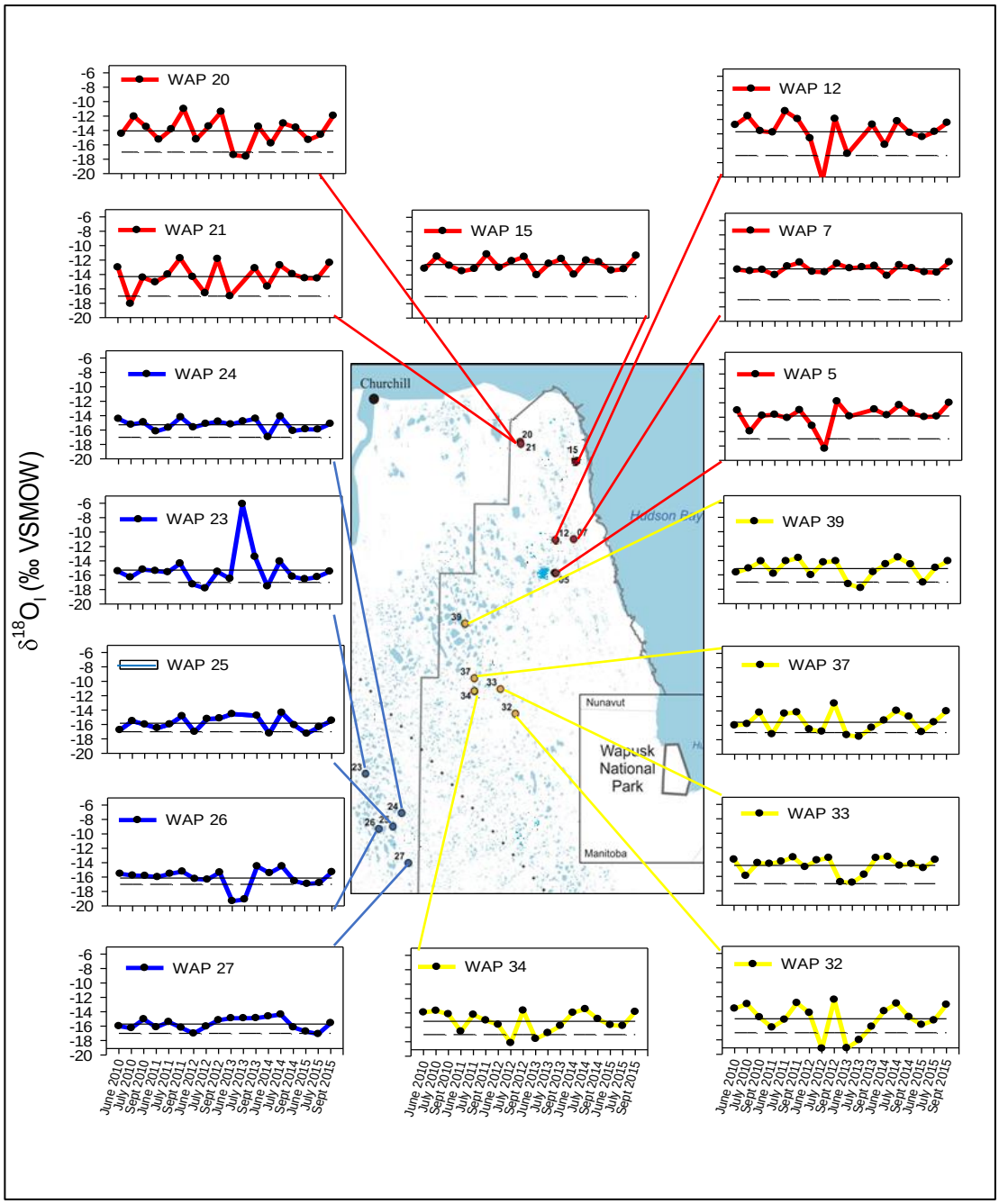

Figure 10. Pond $\delta^{18}O_l$ versus time. Solid black lines represent mean $\delta^{18}O_l$ values for each pond. Dashed black lines represent mean annual isotope composition of precipitation (δ_P).

Table 6. Mean $\delta^{18}O_I$ and E/I values, and standard deviations for ponds sampled between 2010 and 2015. Red labels indicate coastal fen ecozone, blue labels indicate the boreal spruce ecozone and yellow labels indicate the peat plateau ecozone.

Pond	Mean $\delta^{18}O_I$‰	Standard Deviation $\delta^{18}O_I$	Mean E/I	Standard Deviation E/I
WAP05	-13.83	1.56	0.40	0.48
WAP07	-12.71	0.56	0.19	0.13
WAP12	-13.71	2.28	0.45	0.56
WAP15	-12.56	0.91	0.15	0.11
WAP20	-14.05	1.86	0.24	0.24
WAP21	-14.29	1.79	0.39	0.45
n=6				
Avg	**-13.54**	**1.49**	**0.30**	**0.32**
WAP23	-15.28	2.56	0.23	0.33
WAP24	-15.26	0.76	0.11	0.07
WAP25	-15.83	0.94	0.21	0.34
WAP26	-16.13	1.31	0.12	0.13
WAP27	-15.70	0.82	0.11	0.04
n=5				
Avg	**-15.64**	**1.28**	**0.15**	**0.18**
WAP32	-15.06	2.08	0.40	0.50
WAP33	-14.47	1.14	0.22	0.32
WAP34	-15.16	1.43	0.29	0.25
WAP37	-15.56	1.38	0.16	0.13
WAP39	-15.11	1.28	0.12	0.04
n=5				
Avg	**-15.07**	**1.21**	**0.23**	**0.24**

Evaporation to Inflow Ratios

Evaporation to inflow (E/I) ratios were calculated for ponds using pond water isotope compositions (δ_L), input water isotope composition (δ_I) and the isotope composition of evaporated vapour (δ_E). E/I ratios provide a useful metric of pond water balances. Ponds with an E/I =1 represent a water balance in which evaporation equals inflow. Ponds with E/I values <1 indicate more input than evaporation whereas E/I values >1 indicate more influence from evaporation on pond water balance, where E/I values >1.5 indicate very strongly influenced by evaporation. Ponds exhibit a systematic pattern throughout the ice-free season which is observed in the E/I ratios. Data shows that E/I ratios are typically low during the spring thaw, increase during mid-season and decrease during late season, however some variability exists throughout sampling years as well as among ecozones.

All ponds have mean E/I values that fall below 1 (Table 6). Table 6 shows the six-year mean E/I values for ponds in all ecozones as well as the standard deviation for each pond. Temporal patterns of E/I values were based on the six-year mean and used to categorize ponds where greater than 50% of the inflow has evaporated during mid-ice-free-season (E/I > 0.5; Figure 11). Ponds that display this feature during mid-ice-free season for more than one consecutive year include: WAP 5, 12, 21, 32 and 34. Coastal

fen and peat plateau ponds show the greatest variability in E/I ratios throughout the ice-free season and are more influenced by evaporation as they have higher E/I ratios during summer months. Ponds that have an E/I >1 may experience net water level drawdown, which is evident for some coastal fen and peat plateau ponds during July 2010-2013. However, by the September sampling period, all ponds had E/I values below 1, indicating that the input derived during late-season precipitation resulted in ponds with a positive water balance (Figure 11).

Ponds in the boreal spruce ecozone have the smallest amount of variability in E/I ratios, with only slight increases during July months. Lower E/I ratios indicate that evaporation may be offset by snowmelt as vegetation entraps wind distributed snow and delays spring melt (Figure 11). Additionally, there may be less influence from evaporation on ponds in the boreal spruce ecozone as they are typically larger and deeper than ponds in the coastal fen and peat plateau ecozones. During July 2013, however, WAP 23, 25, and 26 all display E/I ratios above 0.5 indicating that evaporation had a strong influence on some boreal spruce pond water balances (Figure 11).

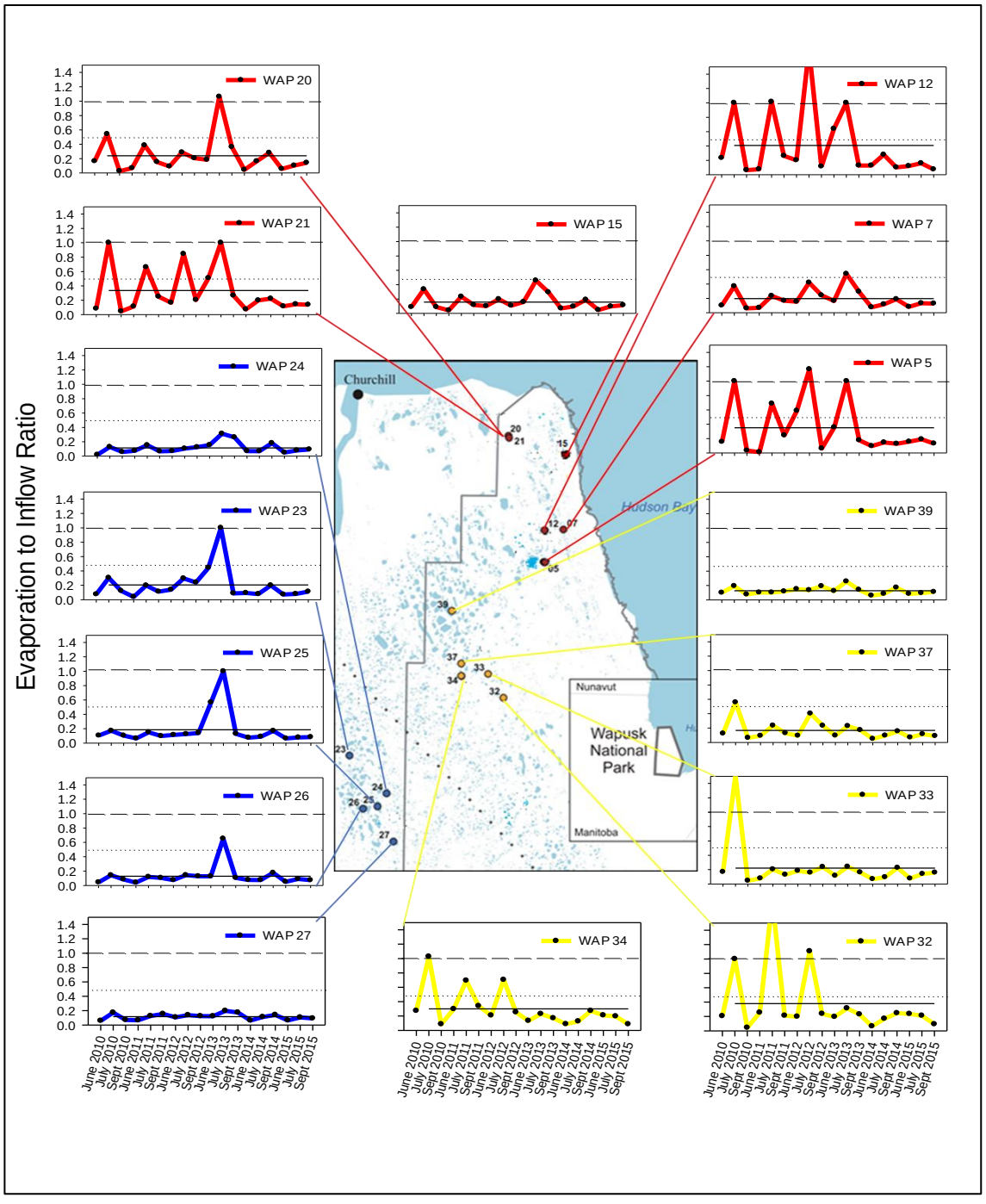

Figure 11. Evaporation to Inflow (E/I) ratios plotted versus sampling time for all ponds. Solid black line represents individual pond E/I mean, dashed line shows E/I = 1 and dotted line represents E/I = 0.5. Ponds plotting with values < 1 = more input than evaporation.

Chapter Four

Discussion

As northern landscapes are displaying changes in lake and pond water balances as a response to climate change (Rowland *et al*., 2010; Carroll *et al*., 2011; Vincent *et al*., 2011), it is critical to implement long-term monitoring to assess these changes now and in the future. While numerous studies have been conducted on the changing water balances of thermokarst landscapes (e.g., Smith *et al*., 2005; Riordan *et al*., 2006; Plug *et al*., 2008), there remains a lack of long-term monitoring on lake water balances to track responses to climate change (Rouse, 2000; Turner *et al*., 2010). Implementing and maintaining a sustainable long-term monitoring program involves collaboration between multiple stakeholders and authorities which can be difficult, especially in remote areas and multiple jurisdictions. An ongoing partnership among Parks Canada, Wilfrid Laurier University and the University of Waterloo has provided training and protocols for hydrological monitoring (based on Tondu *et al*., 2013; White *et al*., in preparation) within Wapusk National Park. Results from the monitoring program can be incorporated into the hydrological component of the State of the Park Report that Parks Canada is required by federal government to produce every ten years.

The approach presented in this study uses water isotope tracers as a monitoring tool to evaluate pond hydrological status and change in a northern thermokarst landscape, Wapusk National Park. To determine the hydrological influences on pond water balance, water isotope tracers were compared annually, seasonally and by ecozone using a six-year data set. Additionally, a mass-balance isotope model was used to characterize the role of input water as δ_I (i.e., snowmelt and rainfall) to ponds and evaporation to inflow (E/I) ratios to assess key features of pond water balances as per Yi et al. (2008). Results demonstrate the diversity of pond hydrological conditions in WNP. Variability can be explained by differences in catchment characteristics, as well as differences in seasonal and annual meteorological conditions.

It was critical to assess two isotope frameworks to determine the one that most accurately represented meteorological conditions within WNP to evaluate pond water balances. Using an evaporation pan to capture isotope values of a simulated terminal pond at isotopic and hydrologic steady state within the Churchill region was the preferred method for establishing the isotope framework. The evaporation pan data formed the *Pan Framework* for evaluating isotope composition of ponds and for calculating δ_I and E/I

values. The *Pan Framework* was used because the alternate *Gonfiantini Framework* did not accurately capture the isotope composition of pond water isotope values. This was evident as pond water isotope values plotted past δ^* on the *Gonfiantini Framework* when in fact ponds were not observed to be desiccated during sampling.

Seasonal Evolution of Pond Water Balances

Pond water isotope composition (δ_L) values were superimposed on the *Pan Framework* and a systematic pattern in pond water balance evolution is evident in most ponds during the ice-free season. δ_L values are low during early ice-free season due to snowmelt. Increase in δ_L values occurs during mid-ice-free season due to evaporation. Depletion of δ_L values at the end of the ice-free typically occurs due to the influence of rainfall. These seasonal patterns lead to a wet-dry-wet pattern in pond water balance. Ponds in the coastal fen and peat plateau ecozones are evidently more influenced from summer evaporation than ponds in the boreal spruce ecozone as δ_L values in the former become more enriched during mid-ice-free season. Lower amounts of snowfall than climate normal (1980-2010) during all six-years may have contributed to enriched δ_L values during mid-ice-free seasons.

Patterns in δ_L values in ponds near Churchill, Manitoba have previously been measured, with ponds being more isotopically depleted during early and late ice-free seasons than mid-ice-free-season as a result of precipitation (Wolfe *et al*., 2011a; Light, 2011; Farquharson, 2013). In addition to the data in this thesis, one study found that even with pond desiccation during mid-ice-free season in WNP due to less snowpack, late ice-free season precipitation replenished pond water balance (Bouchard *et al*., 2013). Additionally, studies in other Arctic regions have found relations between pond water balance with spring thaw and from evaporation and precipitation throughout the ice-free season (Bowling *et al.*, 2003; Woo and Guan, 2006).

Yearly and seasonal data indicate that ponds within the coastal fen and peat plateau ecozones appear to be more sensitive to evaporation than ponds in the boreal spruce ecozone. During 2010 – 2015, most ponds in the boreal spruce ecozone show relatively stable δ_L values. Coastal fen and peat plateau δ_L values show greater inter-seasonal variability and plot around and beyond δ_{SSL} on the LEL during 2010 - 2013 (Figure 8). Through 2014 and 2015, ponds in the coastal fen and peat plateau ecozones display less seasonal variability in δ_L values than previous years as ponds enrich during mid-season

and maintain δ_L values into late-season. This may be a result of higher than climate normal precipitation events that occurred in the ice-free season during these years (Table 2, 3). Mid-ice-free-season increase in δ_L values may be attributed to lower than climate normal average values of June rainfall in addition to lower than climate normal ice-on snowfall (Table 2). Late ice-free season rainfall is likely responsible for replenishing pond water balance and depletion of δ_L values during 2010 to 2012.

Snowmelt and Rainfall

Seasonal changes in water isotope composition in WNP and studies on ponds in other northern regions have indicated that rainfall is an important contributor for replenishing pond water balances *(*Yi *et al.,* 2008; Bouchard *et al.,* 2013; White *et al.,* 2014). Some studies in northern landscapes have indicated snowmelt is a contributing source of input to ponds at the beginning of the ice-free season (Bowling *et* al., 2003, Bouchard *et al*., 2013). In WNP, most ponds plot above δ_P during most sampling times indicating rainfall as the main source of input (Figure 8). However, some ponds plot below δ_P during June sampling, indicating that they are more influenced from snowmelt than rainfall during the early ice-free season (Figure 8).

All ponds in each ecozone show much less variability in δ_I during the 2014 and 2015 ice-free seasons compared to 2010 to 2013 (Figure 10). Both 2014 and 2015 experienced higher than climate normal precipitation during the mid-ice-free season, which indicates that summer evaporation may have been offset by higher precipitation amounts. Farquharson (2013) indicated that these 16 ponds during 2010 – 2012 were influenced by late ice-free season precipitation. Due to late ice-free precipitation ponds were isotopically depleted before ice-cover and therefore had influence from rainfall in addition to snowmelt during early sampling. Given that an increase in ice-free precipitation and a decrease in winter precipitation are predicted for the Churchill region (Macrae *et al*., 2014) ponds may experience changes in their hydrological conditions. Additionally, a study by Derksen and Brown (2012) has shown reduction in snow cover may lead to ponds in the Arctic becoming more rainfall-dominated. Bouchard *et al.* (2013) found that a decrease in snowmelt runoff may lead to an increase in pond desiccation in WNP. Data over the six years may suggest that such predicted changes may already be influencing pond water balances in WNP.

Variability in δ_I values may be influenced by catchment characteristics (e.g., differences between forested areas and non-forested). Previous studies

(Turner *et al*., 2014) have shown a relationship between thermokarst lake δ_I values and catchment vegetation. Forested catchments may capture wind-distributed snow and lead to enhanced snowmelt runoff to lakes. Seasonal variability in δ_I values are most evident in the coastal fen ecozone (Figure 10). Ponds in the coastal fen ecozone have δ_I values that plot relatively higher than δ_P, which indicates that the dominant input source is rainfall. As ponds in the coastal fen ecozone have the least amount of vegetation in their catchment compared to peat plateau and boreal spruce, less snowpack is captured here. Additionally, due to coastal fen ponds being more exposed than ponds with forested catchments, snow distribution from wind is likely. Ponds in the peat plateau ecozone display variability in δ_I values, however they plot closer to δ_P than ponds in the coastal fen, with some pond δ_I values plotting below δ_P during certain sampling times. These δ_I values indicate that ponds in the peat plateau are highly influenced by input of rainfall, however have more influence from snowmelt than ponds in the coastal fen ecozone. Boreal spruce ponds have much less variability in pond water isotope composition and δ_I values, which may be a result of drawn-out spring snowmelt due to lingering snow pack in forested areas. This is substantiated by visible snowpack within forested areas surrounding boreal forest ponds

during June sampling. As surface air temperatures continue to rise, an increase in vegetation in pond catchments has also been recorded in some regions (Jia *et al*., 2009; Turner *et al*., 2014). Additionally, as air temperatures increase, the dynamics of Arctic wetlands have been observed to change with some wetlands growing in size and some shrinking (Smith *et al*., 2005; Hinzman *et al*., 2005; Rowland *et al*., 2010. A general increase in vegetation cover could eventually shift rainfall-dominated ponds to snowmelt-dominated. However, this may be unlikely to occur with predictions of less snowfall and increase in summer rainfall.

Evaporation to Inflow

As ponds in WNP have high surface-area-to-depth ratios, they are susceptible to influence from evaporation. Ponds that possess low E/I ratios and low seasonal variability indicate they are the least sensitive to vapour loss, whereas E/I ratios with high values and variability indicate ponds that are more susceptible to evaporation. Ponds in the coastal fen and peat plateau show a great amount of seasonal and yearly E/I ratio variability as well as high E/I ratios during mid-ice-free season during 2010 - 2013 (Figure 12). This indicates these ponds are influenced strongly from evaporation and are sensitive to vapour loss. A few ponds in these ecozones display E/I ratios

that indicate net level drawdown (E/I >1) during summer months, including some ponds that desiccated. However, these ponds tend to be replenished by late season rainfall. Meteorological conditions show lower than climate normal total rainfall for June 2010 to 2013, which may have led to higher E/I ratios in ponds in the coastal fen and peat plateau ecozones during these ice-free seasons (Table 2). In contrast, E/I ratios during 2014 and 2015 remain relatively stable over all sampling periods in all three ecozones, which may be due to higher than climate normal rainfall levels during early ice-free season in 2014 and July 2015 (Table 2, Figure 11). E/I ratios in the boreal spruce ponds remain relatively stable over all sampling times and years, aside from July 2013, indicating that these ponds have a relatively stable water balance and are more resilient to changes in precipitation (Figure 12). Boreal spruce ponds may be less influenced by summer evaporation due to their larger size and also as a result of drawn out snowmelt. If less snowpack and less early-ice-free season rainfall occur due to climate change, ponds in the boreal spruce ecozone may shift to become more evaporation-dominated. Although the boreal spruce ponds seem more resilient to meteorological conditions than ponds in the coastal fen and peat plateau, dry conditions in 2013 appear to have influenced a response in isotope composition.

As some arctic ponds have experienced changes throughout the North by way of desiccation and reduced water levels (Smol and Douglas, 2007), the continuation of monitoring ponds using water isotope compositions and calculating E/I ratios is critical to understand changes in pond water balance. Results and previous studies (i.e. Bouchard *et al*., 2013) indicate that lower rainfall amounts during early ice-free season may drive ponds to be more evaporatively enriched during mid ice-free season with the potential for desiccation (Figure 12). With respect to observations made by Bouchard *et al.* (2013), the possibility for ponds to desiccate exists as results show that total ice-on rainfall amounts are lower than climate normal during all six years. Mid-ice-free-season E/I ratios in the coastal fen and peat plateau ecozones are indicative of ponds that are experiencing net level drawdown or evaporation dominance. Additionally, the prediction of declining snowmelt runoff may contribute to increases in the occurrences of pond desiccation (Derkson and Brown, 2012). However, with a predicted increase in rainfall amounts (Macrae *et al*., 2014), ponds may maintain relatively stable E/I ratios meaning they would be less likely to desiccate (Figure 12). It is evident that long-term monitoring of these ponds may provide a better understanding of the long-term implications that climate change will have on pond water balance.

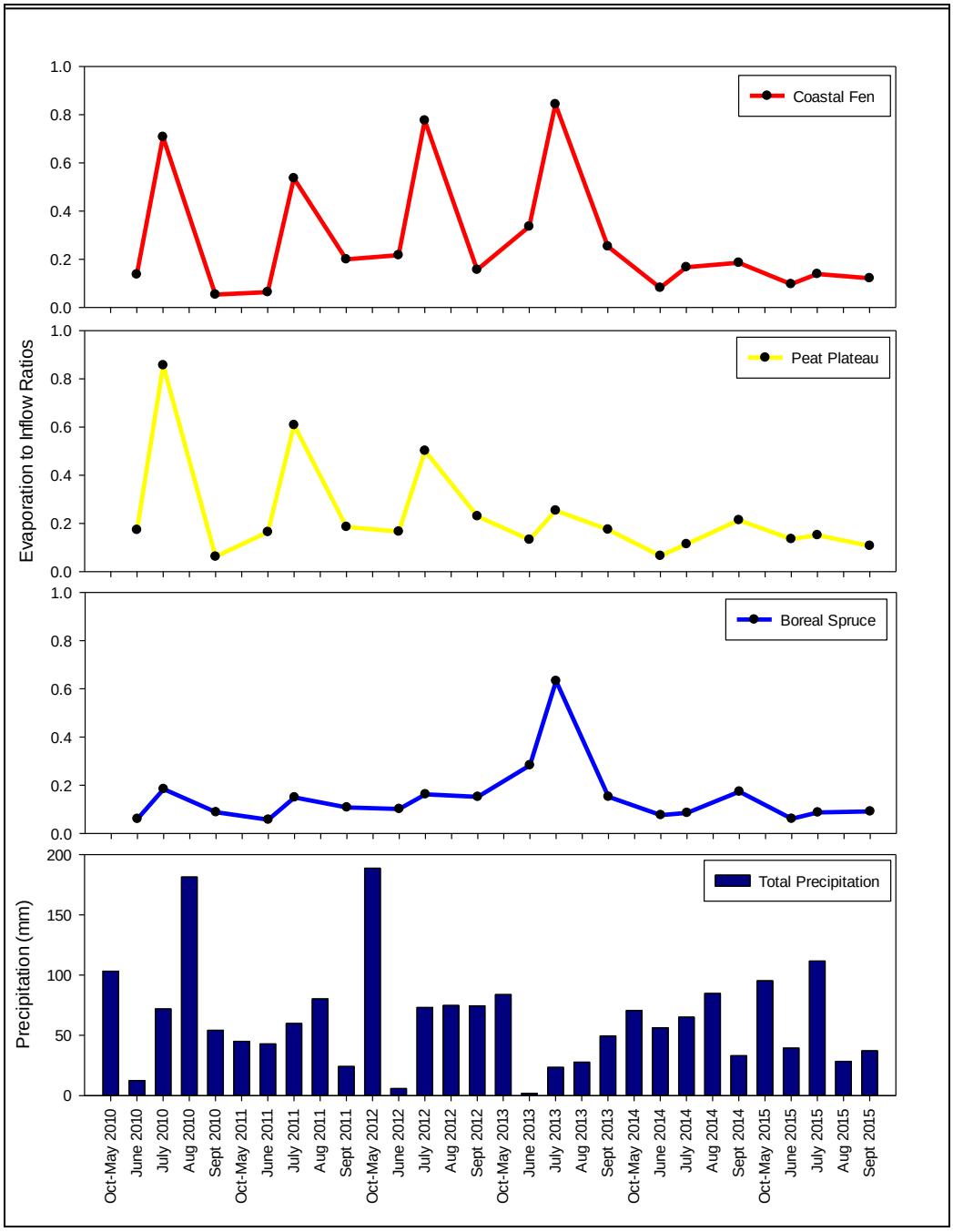

Figure 12. Average pond E/I ratios during 2010 to 2015 compared to total precipitation (mm) values (Environment Canada, 2015).

Conclusion

The knowledge gained from using water isotope tracers and determining input sources and evaporation to inflow ratios contributes to improved understanding of pond water balances in WNP. Results address the research objectives stated in the Introduction of this thesis.

(1) Evaluate two different approaches for developing an 'isotope framework' to be used for current and ongoing long-term hydrological monitoring of ponds in WNP.

Two approaches were taken to determine the most appropriate methods to establish the isotope framework used to interpret pond water isotope data. Firstly, the data were plotted on the *Gonfiantini Framework*, which used the Gonfiantini (1986) equation for δ_{SSL}. Pond water isotope composition plotted past δ^* during times when ponds were not desiccated, which indicated that this framework did not accurately capture atmospheric conditions. The evaporation pan results were used to determine a pond at steady state based on an average value of when the pan equilibrated with atmospheric conditions. Based on pond water isotope compositions plotting in a systematic way on the *Pan Framework* and within LEL parameters, the *Pan Framework* was deemed suitable for the purpose of this study.

The second part of the study focused on estimation of isotope composition of input waters and evaporation to inflow ratios to identify dominant influences on pond water balance. This objective, as stated in the Introduction, is as follows:

(2) Use water isotope tracers measured on a representative suite of ponds in WNP from 2010-2015 and apply an isotope-mass balance model by calculating input water (δ_I) and evaporation to inflow (E/I) ratios to characterize the relative roles of snowmelt, rainfall and evaporation on pond water balances and their spatial, seasonal and annual variability, as well as their relations with meteorological conditions.

Results indicate that there is variability in the hydrological conditions of ponds between ecozones, most notably between the coastal fen and peat plateau ecozone versus the boreal spruce. As snowpack and rainfall change due to climate warming, pond water balance may also be affected. Boreal spruce ponds appear to be less susceptible to changes in rainfall during the ice-free season because pond water balances may be offset by snowmelt during the early ice-free season. Assessing pond sensitivity to evaporation using E/I ratios gives an indication of how evaporation may influence pond

water balance. Some ponds in the coastal fen and peat plateau ecozone have E/I ratios >0.5 during mid-ice-free season indicating that these ponds are more influenced by evaporation than those in the boreal spruce. Ponds in the boreal spruce ecozone maintained relatively stable E/I ratios over most sampling times. These differences indicate that there is hydrological variability within ponds in WNP and future changes in meteorological conditions may influence ponds differently. Dry conditions of 2013 are evidentially influential on ponds and may be indicative of changes to pond water balance due to climate change. It has been demonstrated that water isotope tracers are an excellent tool to monitor variability in pond water balance and capture changes in source water and evaporation. As hydrological changes continue due to climate warming it is necessary to apply methods useful for understanding the long-term changes in pond water balances. The long-term monitoring program in collaboration with WNP will allow for the ability to monitor hydrological changes in WNP. The approaches in this study can readily be adopted into other long-term studies and monitoring programs by other parks and agencies that want to observe trends and changes in lake-rich landscapes in northern regions.

Recommendations

In order to build upon this study and to allow for ongoing hydrological monitoring, several recommendations are made. It is recommended that Parks Canada staff continue to obtain pond water samples during all three sample times to capture the seasonal evolution of pond water balance. Additionally, calculating δ_I values and E/I ratios for ponds is suggested to document key metrics of pond water balances as a response to long-term changes in meteorological (and potentially catchment) conditions. It is also recommended that observations be made on catchment characteristics in each ecozone to determine if there are changes in vegetation.

Results indicate that the *Pan Framework* was most appropriate for interpretation of the water isotope data. Although there are limitations to using the evaporation pan as meteorological conditions throughout WNP are highly variable, the evaporation pan best captures the conditions of the region. Therefore, it is recommended that Parks continue to utilize the evaporation pan as it is easily maintained and represents a consistent, reliable means to obtain estimates of δ_{SSL}. It is recommended to re-assess the framework every 5 years to ensure it accurately reflects local hydro-climatic conditions.

References

ACIA (2004). Arctic Climate Impact Assessment: Summary and Synthesis of the ACIA. Weller, G., Bush, E., Callaghan, T.V., Corell, R., Fox, S., Furgal, C., Hoel, A.H., Huntington, H., Källén, E., Kattsov, V.M., Klein, D.R., Loeng, H., Martello, M.L., MacCracken, M., Nuttall, M., Prowse, T.D., Reiersen, L.O., Reist, J.D., Tanskanen, A., Walsh, J.E., Weatherhead, B., Wrona, F.J. Cambridge University Press, NY, USA.

Barnes, C. J., Allison, G. B. 1983. The distribution of deuterium and ^{18}O in dry soils, 1. Theory. *Journal of Hydrology*, Vol. 60: 141–156.

Beck, I., Ludwig, R., Bernier, M., Levesque, E., Boike, J. 2015. Assessing permafrost degradation and land cover changes (1989-2009) using remote sending data over Umiujaq, Sub-Arctic Quebec. *Permafrost and Periglacial Processes*. Vol. 26: 129-141.

Beever, E., Woodward, A. 2011. Design of ecoregional monitoring in conservation areas of high-latitude ecosystems under contemporary climate change. *Biological Conservation*. Vol. 144: 1258-1269.

Bowen, G.J. 2016. The online isotopes in precipitation calculator, version 2.2. http://www.waterisotopes.org.

Bos, D., and Pellatt, M. 2012. The water chemistry of shallow ponds around Wapusk National Park of Canada, Hudson Bay Lowlands. *Canadian Water Resources Journal*. Vol. 37: 163-175.

Bouchard, F., Turner, K. W., MacDonald, L. A., Deakin, C., White, H., Farquharson, N., Medeiros, A. S., Wolfe, B. B., Hall, R. I., Pienitz, R., Edwards, T. W. D. 2013a. Vulnerability of shallow subarctic lakes to evaporate and desiccate when snowmelt run-off is low. *Geophysical Research Letters*. Vol. 40: 6112-6117.

Bouchard, F., Peinitz, R., Ortiz, J.D., Francus, P., Laurion, I. 2013b. Paleolimnological conditions inferred from fossil diatom assemblages and derivative spectral properties of sediments in thermokarst ponds of subarctic Quebec, Canada. *Boreas.* Vol. 42: 575-595.

Bowling, L.C., Kane, L.D., Gieck, R.E., Hinzman, L.D., Lettenmaier, D.P. 2003. The role of surface storage in a low-gradient Arctic watershed. *Water Resources Research.* Vol. 39: 1-13.

Brock, B.E., Wolfe, B.B., Edwards, T.W.D. 2007. Characterizing the hydrology of shallow floodplain lakes in the Slave River Delta, NWT, using water isotope tracers. *Arctic, Antarctic and Alpine Research.* Vol. 39: 388-401.

Brock, B.E., Wolfe, B.B.., Edwards, T.W.D. 2008. Spatial and temporal perspectives on spring break-up flooding in the Slave River Delta, NWT. *Hydrological Processes* Vol. 22: 4058-4072.

Carroll, M. L., Townshend, J. R. G., DiMiceli, C. M., Loboda, T., Sohlberg, R. A. 2011. Shrinking lakes of the Arctic: spatial relationships and trajectory of change. *Geophysical Research Letters.* Vol. 38: L20406

Chapin, F. S., Sturm, M., Serreze, M. C., McFadden, J. P., Key, J. R., Lloyd, A. H., McGuire, A. D., Rupp, T. S., Lynch, A. H., Schimel, J. P., Beringer, J., Chapman, W. L., Epstein, H. E., Euskirchen, E. S., Hinzman, L. D., Jia, G., Ping, C-L., Tape, K. D., Thompson, C. D. C., Walker, D. A., Welker, J. M. 2005. Role of land-surface changes in arctic summer warming. *Science*. Vol. 310: 657-660.

Clark, I.D., and Fritz, P. 1997. *Environmental Isotopes in Hydrogeology*. Boca Ranton, Florida, CRC Press. 328.

Coleman, M.L., Shepherd, T.J., Durham, J.J., Rouse, J.E., Moore, G.R. 1982. Reduction of water with zinc for hydrogen and isotope analysis. *Analytical Chemistry*. Vol. 54: 993-995.

Coplen, T. B. 1996. New guidelines for reporting stable hydrogen, carbon, and oxygen isotope-ratio data. *Geochimica et Cosmochimica Acta*, Vol. 60: 3359–3360.

Craig, H. 1961. Isotopic variations in meteoric waters. *Science.* Vol. 133: 1702-1703.

Craig, H., and Gordon, L. J. 1965. Deuterium and oxygen 18 variations in the

ocean and the marine atmosphere. In Tongiorgi, E. (ed.), Stable Isotopes in Oceanographic Studies and Paleotemperatures. Pisa, Italy: *Laboratorio di Geologia Nucleare*. 9–130.

Dansgaard, W. 1964. Stable isotopes in precipitation. *Tellus.* Vol. 16: 436-468.

Derksen, C., and Brown, R. 2012. Spring snow cover extent reductions in the 2008-2012 period exceeding climate model projections. *Geophysical Research Letters.* Vol. 39: 19.

Dredge, L.A., and Nixon, F.M. 1992. Glacial and environmental geology of northern Manitoba. *Geological Survey of Canada Memoirs*. 432.

Edwards, T. W. D., Wolfe, B. B., Gibson, J. J., Hammarlund, D. 2004. Use of water isotope tracers in high latitude hydrology and paleolimnology. In Pienitz, R., Douglas, M. S. V., and Smol, J. P. (eds.), *Long-Term Environmental Change in Arctic and Antarctic Lakes.* Dordrecht, Netherlands: Springer. 187–207.

Environment Canada. 2015. Canadian Climate Normals 1981-2010. http://climate.weather.gc.ca/climate_normals/results_1981_2010_e.html

Epstein, S., and Mayeda, T.K. 1953. Variation of $^{18}O/^{16}O$ ratio in waters from natural sources. *Geochimica et Cosmochimica Acta*, Vol. 4: 212-224.

Farquharson, N. 2013. Characterizing the roles of hydrological processes, climate change and Lesser Snow Geese on ponds in Wapusk National Park using isotopic methods. *Wilfrid Laurier University*. MSc Thesis.

Gagnon, A., and Gough, W. 2005. Climate change scenarios for the Hudson Bay region. *Climate Change*. Vol. 69: 269-297.

Gibson, J.J, Edwards T.W.D., Bursey, G. 1993. Estimating evaporation using stable isotope: Quantitative results and sensitivity analysis for two catchments in northern Canada. *Nordic Hydrology*. Vol. 24: 79-94.

Gibson, J.J., Edwards, T.W.D., Prowse, T.D. 1999. Pan-derived isotopic composition of atmospheric water vapour and its variability in northern Canada. *Journal of Hydrology*. Vol. 217: 55-74.

Gibson, J. J., and Edwards, T. W. D. 2002. Regional water balance trends and evaporation-transpiration partitioning from a stable isotope survey of lakes in northern Canada. *Global Biogeochemical Cycles.* Vol. 16: 1–9.

Gibson, J.J., Birks, S.J., Edwards, T.W.D. 2008. Global precipitation of δ_A and δ^2H-$\delta^{18}O$ evaporation slopes for lakes and soil water accounting for seasonality. *Global Biogeochemical Cycles.* Vol. 22: 1-12.

Gonfiantini, R. 1986. Environmental isotopes in lake studies. In Fritz, P., and Fontes, J. C. (eds.), *Handbook of Environmental Isotope Geochemistry*. New York: Elesvier. Vol. 2: 113–168.

Gough,W. A. and Leung, A. 2002. Nature and fate of Hudson Bay permafrost. *Regional Environmental Change*. Vol. 2: 177-184.

Horita, J., and Wesolowski, D. J. 1994. Liquid-vapor fractionation of oxygen and hydrogen isotopes of water from the freezing to the critical temperature. *Geochimica et Cosmochimica Acta*. Vol. 58: 3425–3437.

Johnson, K., Fairfield, L., and Taylor, R., 1987. *Wildflowers of the Hudson Bay Region*. Winnipeg, Canada: Manitoba Museum of Man and Nature. 400 pp.

Jorgenson, M. T., Shur, Y. L., and Pullman, E. R., 2006. Abrupt increase in permafrost degradation in Arctic Alaska. *Geo-physical Research Letters*. Vol. 33: 2.

Karlsson, J., Bring, A., Peterson, G. D., Gordon, L.J., Destourini, G. 2011. Opportunities and limitations to detect climate-related regime shifts in inland Arctic ecosystems through eco-hydrological monitoring. *Environmental Research Letters*. Vol. 6: 14-15.

Kaufman, D., Schneider, D.P., McKay, N.P., Ammann, C.M., Bradley, R.S.,

Briffa, K.R., Miller, G.H., Otto-Bliesner, B.L., Overpeck, J.T., Vithner, B.M. and Arctic Lakes 2K Project Members. 2009. Recent warming reverses long-tern arctic cooling. *Science*. Vol. 325: 1236-1239.

Keatley B.E., Douglas M.S.V., Smol J.P. 2006. Early-20th century environmental changes inferred using subfossil diatoms from a small pond on Melville Island, N.W.T., Canadian High Arctic. *Hydrobiologia*. Vol. 553: 15-26.

Macrae, M. L., Brown, L., Duguay, C. R., Parrott, J. A., Petrone, R. M. 2014. Observed and projected climate change in the Churchill region of the Hudson Bay Lowlands and implications for pond sustainability. *Arctic, Antarctic and Alpine Research.* Vol. 46: 272–285.

MacDonald, L.A., Turner, K.W., Balasubramaniam, A.A., Wolfe, B.B., Hall, R.I., Sweetman, J.N. 2012. Tracking hydrological responses of a thermokarst lake in the Old Crow Flats (Yukon Territory, Canada) to recent climate variability using aerial photographs and paleolimnological methods. *Hydrological Processes.* Vol. 26: 117-129.

MacDonald, L.A., Wolfe, B.B., Turner, K.W., Anderson, L., Arp, C.D., Birks, S.J., Bouchard, F., Edwards, T.W.D., Farquharson, N., Hall, R.I., McDonald, I., Narancic, B., Ouimet, C., Pienitz, R., Tondu, J., White. H. 2017. A synthesis of thermokarst lake water balance in high-latitude regions of North America from isotope tracers. *Arctic Science* (in press).

Malmstrom, V.H. 1969. A new approach to the classification of climate. Journal of Geography. Vol. 68: 351-357.

Markham, W. E. 1986. *The ice cover*. In Martini, I. P. (ed.), Canadian Inland Seas, Elsevier, Amsterdam.

Mezquida J.A., Fernández A., Lucio J.V. & Yangüas M.A.M. 2005. A framework for designing ecological monitoring programs for protected areas: a case study of the Galachos del Ebro Nature Reserve (Spain). *Environmental Management.* Vol. 35: 20-33.

Parks Canada, 2008: Ecological Integrity Monitoring Action Plan for Wapusk National Park of Canada 2008–2013. Churchill, Manitoba: Parks Canada Agency, Manitoba Field Unit.

Prowse, T. D., Wrona, F. J., Reist, J. D., Gibson, J. J., Hobbie, J. E., Levesque, L M. J., Vincent, W. F. 2006. Climate change effects on hydroecology of Arctic freshwater ecosystems. *Ambio.* Vol. 3: 347–358.

Prowse, T.D., Furgal, C., Wrona, F.J., and Reist, J.D. 2009. Implications of climate change for northern Canada: freshwater, marine, and terrestrial ecosystems. *Ambio*. Vol. 35: 282-289.

Riordan, B., Verbyla, D., McGuire, A.D. 2006. Shrinking ponds in subarctic Alaska based on 1950-2002 remotely sensed images. *Journal of Geophysical Research.* Vol: 111.

Rouse, W.R. 1991. Impacts of Hudson Bay on the terrestrial climate of the Hudson Bay Lowlands. *Arctic and Alpine Research.* Vol. 23: 24-30.

Rouse, W.R., Douglas, M.V., Hecky, R.E., Hershey, A.E., Kling, G.W., Lesack, L., Marsh, P., McDonald, M., Nicholson, B.J., Roulet, N.T., Smol, J.P. 1997. Effects of climate change on the freshwaters of Arctic and Subarctic North America. *Hydrological Processes.* Vol: 11: 873-902.

Rowland, J. C., Jones, C. E., Altmann, G., Bryan, R., Crosby, B. T., Geernaert, G. L., Hinzman, L. D., Kane, D. L., Lawrence, D. M., Mancino, A., Marsh, P., McNamara, J. P., Romanovsky, V. E., Toniolo, H., Travis, B. J., Trochim, E., and Wilson, C. J., 2010. Arctic landscapes in transition: responses to thawing permafrost. *EOS, Transactions, American Geophysical Union*. Vol. 91(26): 229–236.

Schindler, D. W., and Smol, J. P., 2006. Cumulative effects of climate warming and other human activities on freshwaters of Arctic and subarctic North America. *Ambio*. Vol. 35: 160–168.

Sannel, A. B. K., and Kuhry, P. 2011. Warming-induced destabilization of peat plateau/thermokarst lake complexes. *Journal of Geophysical Research*. Vol. 116.

Sella, G. F., Stein, S., Dixon, T. H., Craymer, M., James, T. S., Mazzotti, S., Dokka, R. K. 2007. Observation of glacial isostatic adjustment in "stable" North America with GPS. *Geophysical Research Letters*. Vol. 34: 105-111.

Smith, L.C., Sheng, Y., MacDonald, G.M., Hinzman, L.D. 2005. Disappearing Arctic lakes. *Science.* Vol. 308: 1429.

Smol, J. P., and Douglas, M. S. V., 2007. Crossing the final ecological threshold in high Arctic ponds. *Proceedings of the National Academy of Sciences of the United States of America.* Vol. 104: 12395–12397.

Smol, J.P., and Douglas, M. S. V. 2007. From controversy to consensus: making the case for recent climate change in the Arctic using lake sediments. *Frontiers in Ecology and the Environment.* Vol. 5: 466-474.

Thornthwaite, C. 1948. An approach toward a rational classification of climate. *The Geographical Review.* Vol. 38: 1–94.

Tondu, J. M. E., Turner, K. W., Wolfe, B. B., Hall, R. I., Edwards, T. W. D., McDonald, I. 2013. Using water isotope tracers to develop the hydrological component of a long-term aquatic ecosystem monitoring program for a northern lake-rich landscape. *Arctic, Antarctic and Alpine Research.* Vol. 45: 594-614.

Turner, K.W., Wolfe, B.B., Edwards, T.W.D. 2010. Characterizing the role of hydrological processes on lake water balances in the Old Crow Flats, Yukon Territory, Canada using water isotope tracers. *Journal of Hydrology*. Vol. 386: 103-117.

Turner, K.W., Wolfe, B.B., Edwards, T.D., Lantz, T.C., Hall, R.I, Larocque, G. 2014. Controls on water balance of shallow thermokarst lakes and their relations with catchment characteristics: a multi-year, landscape-scale assessment based on water isotope tracers and remote sensing in Old Crow Flats, Yukon (Canada). *Global Change Biology.* Vol. 20: 1585-1603.

Webber, P. J., Richardson, J. W., Andrew, J. T. 1970. Post-glacial uplift and substrate age at Cape Henrietta Maria, southeastern Hudson Bay, Canada. *Canadian Journal of Earth Sciences*. Vol. 7: 317– 325.

Wolfe, B.B., Falcone, M.D., Clogg-Wright, K.P., Mongeon, C.L., Yi, Y., Brock, B.E., St. Amour, N.A., Mark, W.A., Edwards, T.W.D. 2007. Progress in isotope paleohydrology using lake sediment cellulose. *Journal of Paleolimnology.* Vol. 37: 221-231.

Wolfe, B.B., Light, E.M., Macrae, M.L., Hall, R.I., Eichel, K., Jasechko, S., White, J., Fishback, L., Edwards, T.W.D. 2011a. Divergent hydrological responses to 20th century climate change in shallow tundra ponds, western Hudson Bay Lowlands. *Geophysical Research Letters*. Vol. 38: L23402.

Wolfe, B. B., Humphries M. M., Pisaric M. F. J., Balasubramaniam A. M., Burn C. R., Chan L., Cooley D., Froese D. G., Graupe S., Hall R. I., Lantz T., Porter T. J., Roy-Leveillee P., Turner K. W., Wesche S. D., and Williams M. 2011b. Environmental change and traditional use of the Old Crow Flats in Northern Canada: an IPY opportunity to meet the challenges of the new northern research paradigm. *Arctic* Vol. 64(1):127-135.

White, H. 2015. Contemporary and paleolimnological approaches for assessing the effects of climate change on the hydrology of shallow subarctic lakes and ponds in Wapusk National Park, Manitoba. PhD in Progress, *Wilfrid Laurier University*.

White, H., Turner, K., Tondu, J., MacDonald, L.A., Ouimet, C., MacDonald, I., Venkiteswaran, J., Wolfe, B.B., and Hall, R.I. (in preparation) 2016. Development and application of hydrological monitoring in lake-rich landscapes in Canada's subarctic National Parks using water isotopes. In preparation for Environmental Monitoring and Assessment.

Winter, T.C., and Woo, M.K. 1990. Hydrology of lakes and wetlands. *In* Wolmand, M.G., and Riggs, H.C. (eds.), *Surface Water Hydrology.* Boulder, Colorado: Geological Society of America, The Geology of North America. Vol. 0-1: 159-187.

Vaughan, H., Brydges, A., Fenech, A., Lumb, A. 2001. Monitoring long-term ecological changes through the ecological monitoring and assessment network: Science-based and policy relevant. *Environmental Monitoring and Assessment*. Vol. 67: 3-28.

Vincent, W.F., Callaghan, T.V., Dahl-Jensen, D., Johansson, M., Kovacs, K.M., Michel, C., Prowse, T., Reist, J.D., Sharp, M. 2011. Chapter 11: Effects of climate change on snow, water, ice, and permafrost in Arctic ecosystems—Synthesis. In Snow, Water, Ice and Permafrost in the Arctic (SWIPA), Arctic Monitoring and Assessment Programme (AMAP), Oslo.

Yi, Y., Brock, B. B., Falcone, M.D., Wolfe, B.B., Edwards, T.W.D. 2008. A coupled isotope tracer method to characterize input water to lakes. *Journal of Hydrology*. Vol. 350: 1-13.

Appendix A

Pond Water Isotope Composition of $\delta^{18}O_L$, $\delta^{2}H_L$, $\delta^{18}O_I$, $\delta^{2}H_I$, and E/I

Date	Pond Name	$\delta^{18}O_L$	$\delta^{2}H_L$	$\delta^{18}O_I$	$\delta^{2}H_I$	E/I
June 2010	WAP05	-9.43	-80.99	-13.06	-94.50	0.15
June 2010	WAP07	-10.13	-82.88	-12.80	-92.43	0.10
June 2010	WAP12	-8.30	-75.89	-12.76	-92.08	0.23
June 2010	WAP15	-10.63	-85.81	-13.13	-95.08	0.08
June 2010	WAP20	-10.14	-87.56	-14.46	-105.71	0.16
June 2010	WAP21	-10.66	-85.51	-13.01	-94.08	0.08
June 2010	WAP23	-12.71	-101.54	-15.44	-113.52	0.07
June 2010	WAP24	-13.68	-102.49	-14.44	-105.59	0.01
June 2010	WAP25	-12.88	-105.79	-16.77	-124.22	0.10
June 2010	WAP26	-13.79	-106.67	-15.54	-114.38	0.04
June 2010	WAP27	-13.62	-107.29	-16.00	-118.01	0.05
June 2010	WAP32	-9.09	-81.14	-13.64	-99.15	0.20
June 2010	WAP33	-9.60	-83.27	-13.67	-99.36	0.16
June 2010	WAP34	-8.50	-79.23	-13.92	-101.36	0.27
June 2010	WAP37	-11.92	-99.38	-16.02	-118.17	0.122
June 2010	WAP39	-12.20	-99.77	-15.65	-115.20	0.09
July 2010	WAP05	-4.76	-63.35	-15.96	-117.73	2.21
July 2010	WAP07	-7.36	-72.76	-13.03	-94.25	0.36
July 2010	WAP12	-1.37	-48.75	-11.53	-82.30	N/A
July 2010	WAP15	-6.91	-67.94	-11.45	-81.67	0.33
July 2010	WAP20	-6.21	-66.70	-12.06	-86.79	0.54
July 2010	WAP21	-4.64	-63.29	-18.07	-134.60	2.92
July 2010	WAP23	-9.29	-87.10	-16.29	-120.38	0.30
July 2010	WAP24	-11.28	-94.52	-15.24	-111.99	0.12
July 2010	WAP25	-10.66	-92.28	-15.51	-114.15	0.17
July 2010	WAP26	-11.34	-96.06	-15.78	-116.24	0.14
July 2010	WAP27	-11.07	-95.83	-16.27	-120.17	0.17
July 2010	WAP32	-3.65	-57.21	-13.02	-94.23	13.91
July 2010	WAP33	-5.27	-66.03	-15.92	-117.40	1.50
July 2010	WAP34	-5.50	-65.71	-13.69	-99.54	1.0
July 2010	WAP37	-7.33	-76.56	-15.81	-116.52	0.55
July 2010	WAP39	-10.07	-88.60	-15.08	-110.65	0.19
Sept 2010	WAP05	-12.56	-95.53	-13.78	-100.26	0.03
Sept 2010	WAP07	-11.01	-86.22	-12.84	-92.75	0.06

Sept 2010	WAP12	-11.53	-90.88	-13.61	-98.89	0.06
Sept 2010	WAP15	-10.31	-83.24	-12.72	-91.76	0.08
Sept 2010	WAP20	-12.55	-94.48	-13.51	-98.14	0.02
Sept 2010	WAP21	-12.73	-98.46	-14.42	-105.38	0.04
Sept 2010	WAP23	-11.38	-94.86	-15.20	-111.63	0.12
Sept 2010	WAP24	-12.78	-100.33	-14.93	-109.49	0.05
Sept 2010	WAP25	-12.35	-101.32	-15.99	-117.95	0.10
Sept 2010	WAP26	-12.72	-102.62	-15.82	-116.63	0.08
Sept 2010	WAP27	-12.50	-99.41	-15.03	-110.29	0.07
Sept 2010	WAP32	-13.18	-101.81	-14.85	-108.82	0.04
Sept 2010	WAP33	-12.49	-96.55	-14.14	-103.16	0.04
Sept 2010	WAP34	-11.46	-92.38	-14.16	-103.32	0.08
Sept 2010	WAP37	-12.08	-95.13	-14.23	-103.84	0.06
Sept 2010	WAP39	-11.66	-92.93	-14.08	-102.68	0.07
June 2011	WAP05	-13.26	-97.73	-13.65	-99.24	0.01
June 2011	WAP07	-11.57	-90.77	-13.56	-98.55	0.06
June 2011	WAP12	-11.59	-91.64	-13.80	-100.47	0.07
June 2011	WAP15	-12.14	-92.71	-13.48	-97.88	0.04
June 2011	WAP20	-13.00	-102.23	-15.27	-112.17	0.06
June 2011	WAP21	-11.78	-96.27	-15.09	-110.72	0.11
June 2011	WAP23	-13.97	-106.90	-15.38	-113.11	0.03
June 2011	WAP24	-13.55	-107.39	-16.18	-119.44	0.07
June 2011	WAP25	-14.09	-110.85	-16.50	-122.03	0.06
June 2011	WAP26	-14.44	-111.01	-16.00	-118.04	0.04
June 2011	WAP27	-13.79	-108.46	-16.15	-119.25	0.06
June 2011	WAP32	-10.18	-91.37	-16.26	-120.13	0.25
June 2011	WAP33	-11.91	-94.37	-14.25	-104.00	0.07
June 2011	WAP34	-9.84	-90.17	-16.57	-122.62	0.29
June 2011	WAP37	-13.90	-111.85	-17.23	-127.84	0.09
June 2011	WAP39	-12.55	-101.75	-15.83	-116.64	0.10
July 2011	WAP05	-6.36	-69.61	-14.11	-102.92	0.68
July 2011	WAP07	-8.24	-74.24	-12.36	-88.92	0.23
July 2011	WAP12	-4.75	-59.11	-10.83	-76.71	1.01
July 2011	WAP15	-8.70	-78.07	-13.16	-95.33	0.23
July 2011	WAP20	-7.73	-75.36	-13.82	-100.61	0.38
July 2011	WAP21	-6.41	-69.74	-14.00	-102.06	0.66
July 2011	WAP23	-10.58	-91.89	-15.57	-114.57	0.19
July 2011	WAP24	-11.40	-95.98	-15.67	-115.43	0.15
July 2011	WAP25	-11.64	-97.86	-15.98	-117.85	0.15
July 2011	WAP26	-11.98	-98.38	-15.54	-114.35	0.11
July 2011	WAP27	-11.74	-96.96	-15.42	-113.36	0.12
July 2011	WAP32	-4.69	-62.43	-15.19	-111.56	1.80

July 2011	WAP33	-9.49	-83.22	-13.93	-101.51	0.20
July 2011	WAP34	-6.38	-69.85	-14.24	-103.94	0.69
July 2011	WAP37	-9.38	-83.76	-14.37	-104.99	0.23
July 2011	WAP39	-11.27	-91.15	-14.28	-102.68	0.10
Sept 2011	WAP05	-8.49	-76.85	-13.01	-94.09	0.24
Sept 2011	WAP07	-8.63	-74.08	-11.81	-84.53	0.16
Sept 2011	WAP12	-7.75	-71.36	-11.94	-85.53	0.26
Sept 2011	WAP15	-8.86	-72.53	-11.15	-79.25	0.11
Sept 2011	WAP20	-8.30	-70.34	-11.01	-78.09	0.15
Sept 2011	WAP21	-7.75	-70.84	-11.74	-83.96	0.25
Sept 2011	WAP23	-11.29	-92.05	-14.36	-104.88	0.11
Sept 2011	WAP24	-12.15	-95.27	-14.21	-103.72	0.06
Sept 2011	WAP25	-11.92	-96.18	-14.83	-108.71	0.09
Sept 2011	WAP26	-12.04	-97.85	-15.24	-111.94	0.10
Sept 2011	WAP27	-11.71	-98.68	-16.20	-119.64	0.15
Sept 2011	WAP32	-8.78	-77.66	-12.87	-93.00	0.21
Sept 2011	WAP33	-10.21	-84.59	-13.34	-96.72	0.13
Sept 2011	WAP34	-8.65	-81.73	-15.04	-110.36	0.33
Sept 2011	WAP37	-10.83	-89.61	-14.19	-103.54	0.12
Sept 2011	WAP39	-10.62	-87.12	-13.63	-99.04	0.11
June 2012	WAP05	-7.09	-74.50	-15.20	-111.67	0.58
June 2012	WAP07	-9.63	-81.70	-13.11	-94.89	0.15
June 2012	WAP12	-9.87	-86.53	-14.61	-106.91	0.20
June 2012	WAP15	-10.42	-84.45	-13.01	-94.09	0.10
June 2012	WAP20	-12.32	-99.16	-15.24	-111.99	0.09
June 2012	WAP21	-10.23	-87.46	-14.34	-104.73	0.16
June 2012	WAP23	-12.68	-105.88	-17.27	-128.17	0.13
June 2012	WAP24	-13.12	-103.87	-15.63	-115.04	0.07
June 2012	WAP25	-13.11	-107.47	-17.02	-126.19	0.11
June 2012	WAP26	-13.55	-107.60	-16.25	-120.04	0.07
June 2012	WAP27	-13.25	-108.10	-17.01	-126.13	0.10
June 2012	WAP32	-9.72	-85.03	-14.25	-104.02	0.19
June 2012	WAP33	-10.20	-88.18	-14.69	-107.55	0.18
June 2012	WAP34	-10.39	-91.13	-15.63	-115.07	0.20
June 2012	WAP37	-13.27	-107.03	-16.54	-122.36	0.09
June 2012	WAP39	-11.61	-97.87	-16.03	-188.28	0.15
July 2012	WAP05	-6.13	-72.06	-18.38	-137.05	1.16
July 2012	WAP07	-7.20	-72.05	-13.18	-95.48	0.42
July 2012	WAP12	-5.55	-69.58	-20.40	-153.23	1.73
July 2012	WAP15	-8.43	-74.27	-12.08	-86.70	0.19
July 2012	WAP20	-8.28	-77.04	-13.43	-97.49	0.28
July 2012	WAP21	-6.53	-73.05	-16.60	-122.82	0.84

July 2012	WAP23	-10.37	-94.94	-17.82	-132.56	0.29
July 2012	WAP24	-11.89	-96.91	-15.13	-111.07	0.10
July 2012	WAP25	-11.56	-95.66	-15.22	-111.84	0.12
July 2012	WAP26	-11.96	-100.24	-16.34	-120.76	0.14
July 2012	WAP27	-11.85	-99.05	-16.04	-118.37	0.13
July 2012	WAP32	-6.42	-74.26	-19.20	-143.62	1.10
July 2012	WAP33	-9.98	-84.87	-13.75	-100.05	0.15
July 2012	WAP34	-7.49	-79.67	-18.18	-135.48	0.70
July 2012	WAP37	-8.86	-85.65	-16.87	-125.00	0.40
July 2012	WAP39	-10.67	-89.12	-14.24	-103.92	0.13
Sept 2012	WAP05	-10.24	-79.46	-11.80	-84.45	0.06
Sept 2012	WAP07	-7.93	-72.27	-12.00	-86.03	0.24
Sept 2012	WAP12	-9.41	-77.09	-11.90	-85.26	0.11
Sept 2012	WAP15	-9.19	-74.88	-11.48	-81.91	0.10
Sept 2012	WAP20	-7.94	-70.64	-11.40	-81.26	0.20
Sept 2012	WAP21	-8.21	-72.77	-11.82	-84.63	0.20
Sept 2012	WAP23	-9.87	-88.45	-15.51	-114.10	0.24
Sept 2012	WAP24	-11.27	-93.28	-14.88	-108.58	0.12
Sept 2012	WAP25	-11.23	-93.97	-15.15	-111.26	0.13
Sept 2012	WAP26	-11.60	-96.13	-15.35	-112.83	0.12
Sept 2012	WAP27	-11.54	-95.41	-15.16	-111.35	0.12
Sept 2012	WAP32	-8.21	-74.37	-12.41	-89.29	0.23
Sept 2012	WAP33	-8.76	-78.99	-13.42	-97.41	0.23
Sept 2012	WAP34	-8.74	-79.46	-13.66	-99.29	0.25
Sept 2012	WAP37	-8.56	-77.08	-12.96	-93.71	0.23
Sept 2012	WAP39	-9.70	-84.52	-14.07	-102.57	0.19
June 2013	WAP05	-8.17	-76.92	-13.87	-101.03	0.35
June 2013	WAP07	-9.43	-79.05	-12.63	-91.07	0.16
June 2013	WAP12	-7.58	-78.61	-16.77	-124.22	0.63
June 2013	WAP15	-10.50	-87.50	-14.03	-102.24	0.15
June 2013	WAP20	-12.41	-104.77	-17.41	-129.34	0.18
June 2013	WAP21	-8.48	-83.70	-17.01	-126.12	0.50
June 2013	WAP23	-8.75	-84.33	-16.49	-121.99	0.44
June 2013	WAP24	-11.42	-94.73	-15.20	-111.61	0.15
June 2013	WAP25	-7.10	-73.21	-14.55	-106.44	0.56
June 2013	WAP26	-15.00	-122.38	-19.33	-144.71	0.12
June 2013	WAP27	-11.79	-95.63	-14.90	-109.25	0.12
June 2013	WAP32	-13.38	-113.37	-19.15	-143.21	0.19
June 2013	WAP33	-13.37	-108.09	-16.79	-124.34	0.11
June 2013	WAP34	-13.58	-111.10	-17.60	-130.80	0.13
June 2013	WAP37	-14.31	-114.16	-17.36	-128.88	0.09
June 2013	WAP39	-13.54	-110.12	-17.28	-128.28	0.12

July 2013	WAP05	-2.72	-55.56	14.56	125.71	N/A
July 2013	WAP07	-6.38	-66.51	-12.47	-89.80	0.54
July 2013	WAP12	-2.28	-52.98	0.62	14.99	N/A
July 2013	WAP15	-6.80	-68.18	-12.45	-89.62	0.45
July 2013	WAP20	-6.19	-71.91	-17.62	-131.00	1.06
July 2013	WAP21	-4.02	-61.60	-26.23	-199.81	4.40
July 2013	WAP23	-3.40	-60.30	-6.09	-38.78	N/A
July 2013	WAP24	-9.05	-82.82	-14.79	-108.35	0.31
July 2013	WAP25	-3.35	-60.31	71.73	583.90	N/A
July 2013	WAP26	-8.37	-85.60	-19.1	-142.82	0.65
July 2013	WAP27	-10.52	-89.87	-14.91	-109.25	0.19
July 2013	WAP32	-10.83	-97.69	-18.02	-134.16	0.31
July 2013	WAP33	-11.13	-97.16	-16.86	-124.91	0.24
July 2013	WAP34	-11.26	-97.68	-16.80	-124.36	0.22
July 2013	WAP37	-11.77	-101.85	-17.58	-130.64	0.22
July 2013	WAP39	-11.48	-100.82	-17.83	-132.63	0.25
Sept 2013	WAP05	-9.47	-80.08	-12.92	-93.39	0.17
Sept 2013	WAP07	-7.86	-72.03	-12.30	-88.40	0.29
Sept 2013	WAP12	-10.03	-81.63	-12.72	-91.72	0.12
Sept 2013	WAP15	-7.56	-69.54	-11.79	-84.31	0.29
Sept 2013	WAP20	-7.93	-75.06	-13.49	-97.90	0.36
Sept 2013	WAP21	-8.59	-77.03	-13.13	-95.04	0.26
Sept 2013	WAP23	-11.32	-89.14	-13.44	-97.52	0.08
Sept 2013	WAP24	-9.39	-83.58	-14.43	-105.47	0.26
Sept 2013	WAP25	-11.56	-94.24	-14.78	-108.20	0.12
Sept 2013	WAP26	-11.80	-94.54	-14.51	-106.06	0.10
Sept 2013	WAP27	-10.85	-91.33	-14.88	-109.07	0.17
Sept 2013	WAP32	-10.88	-94.46	-16.47	-119.34	0.22
Sept 2013	WAP33	-11.68	-97.38	-15.77	-116.15	0.16
Sept 2013	WAP34	-11.54	-96.77	-15.78	-116.22	0.17
Sept 2013	WAP37	-11.92	-99.90	-16.34	-120.72	0.17
Sept 2013	WAP39	-11.96	-98.31	-15.61	-114.84	0.14
June 2014	WAP05	-11.31	-90.05	-13.72	-99.76	0.09
June 2014	WAP07	-11.68	-91.44	-13.68	-99.44	0.07
June 2014	WAP12	-12.04	-98.52	-15.53	-114.21	0.12
June 2014	WAP15	-12.04	-93.85	-13.96	-101.64	0.07
June 2014	WAP20	-14.30	-109.66	-15.80	-116.42	0.04
June 2014	WAP21	-13.41	-105.20	-15.67	-115.36	0.07
June 2014	WAP23	-14.41	-115.13	-17.55	-130.41	0.09
June 2014	WAP24	-14.59	-114.50	-16.97	-125.77	0.07
June 2014	WAP25	-14.66	-115.60	-17.25	-127.97	0.07
June 2014	WAP26	-13.16	-103.42	-15.46	-113.64	0.07

June 2014	WAP27	-12.80	-99.33	-14.64	-107.13	0.06
June 2014	WAP32	-12.28	-95.05	-14.02	-102.14	0.06
June 2014	WAP33	-11.65	-90.48	-13.44	-97.48	0.06
June 2014	WAP34	-11.69	-92.45	-13.98	-101.81	0.08
June 2014	WAP37	-13.77	-105.75	-15.32	-112.57	0.04
June 2014	WAP39	-12.74	-98.59	-14.50	-105.97	0.06
July 2014	WAP05	-9.44	-78.23	-12.34	-88.72	0.14
July 2014	WAP07	-9.76	-78.95	-12.20	-87.58	0.11
July 2014	WAP12	-7.91	-72.23	-12.25	-87.99	0.27
July 2014	WAP15	-9.95	-78.89	-11.99	-85.92	0.09
July 2014	WAP20	-9.68	-81.25	-13.02	-94.15	0.16
July 2014	WAP21	-9.02	-77.78	-12.72	-91.78	0.19
July 2014	WAP23	-11.99	-94.10	-14.10	-102.78	0.07
July 2014	WAP24	-12.21	-95.05	-14.11	102.91	0.06
July 2014	WAP25	-11.98	-94.90	-14.37	-104.93	0.08
July 2014	WAP26	-12.40	-97.17	-14.51	-106.05	0.07
July 2014	WAP27	-11.51	-92.90	-14.38	-105.00	0.11
July 2014	WAP32	-9.58	-80.66	-12.95	-93.60	0.16
July 2014	WAP33	-10.99	-87.32	-13.29	-96.31	0.09
July 2014	WAP34	-10.58	-86.25	-13.46	-97.70	0.12
July 2014	WAP37	-11.54	-91.80	-13.97	-101.79	0.09
July 2014	WAP39	-11.42	-89.97	-13.57	-98.52	0.08
Sept 2014	WAP05	-10.53	-86.05	-13.46	-97.70	0.12
Sept 2014	WAP07	-9.07	-77.71	-12.62	-90.97	0.18
Sept 2014	WAP12	-11.30	-90.43	-13.85	-100.81	0.10
Sept 2014	WAP15	-8.79	-75.45	-12.22	-87.73	0.19
Sept 2014	WAP20	-8.67	-78.59	-13.60	-98.80	0.28
Sept 2014	WAP21	-9.51	-83.03	-13.94	-101.53	0.22
Sept 2014	WAP23	-11.28	-96.53	-16.21	-119.69	0.19
Sept 2014	WAP24	-11.49	-97.33	-16.11	-118.91	0.18
Sept 2014	WAP25	-11.70	-98.28	-16.09	-118.70	0.16
Sept 2014	WAP26	-11.91	-100.44	-15.58	-122.60	0.17
Sept 2014	WAP27	-12.28	-101.29	-16.17	-119.35	0.14
Sept 2014	WAP32	-9.75	-86.16	-14.82	-108.53	0.24
Sept 2014	WAP33	-9.81	-85.71	-14.50	-105.99	0.22
Sept 2014	WAP34	-9.47	-84.91	-14.84	-108.72	0.27
Sept 2014	WAP37	-11.06	-92.08	-14.79	-108.32	0.15
Sept 2014	WAP39	-10.58	-89.22	-14.51	-106.11	0.17
June 2015	WAP05	-9.80	-84.95	-13.96	-101.70	0.15
June 2015	WAP07	-10.67	-86.23	-13.19	-95.48	0.08
June 2015	WAP12	-10.76	-90.23	-14.44	-105.50	0.12
June 2015	WAP15	-11.73	-90.96	-13.40	-97.19	0.04

June 2015	WAP20	-13.03	-102.64	-15.32	-112.53	0.05
June 2015	WAP21	-10.90	-91.06	-14.52	-106.16	0.11
June 2015	WAP23	-13.48	-108.16	-16.56	-122.49	0.07
June 2015	WAP24	-13.69	-107.28	-15.89	-117.09	0.05
June 2015	WAP25	-14.30	-113.98	-17.28	-128.25	0.06
June 2015	WAP26	-14.51	-114.09	-16.94	-125.50	0.05
June 2015	WAP27	-13.90	-110.67	-16.75	-123.97	0.06
June 2015	WAP32	-9.74	-88.72	-15.91	-117.26	0.23
June 2015	WAP33	-11.62	-93.40	-14.27	-104.14	0.07
June 2015	WAP34	-9.99	-89.54	-15.68	-115.44	0.20
June 2015	WAP37	-13.86	-110.93	-16.93	-125.46	0.06
June 2015	WAP39	-13.47	-109.38	-17.06	-126.49	0.08
July 2015	WAP05	-9.27	-82.58	-13.89	-101.10	0.19
July 2015	WAP07	-9.74	-82.82	-13.24	-95.89	0.13
July 2015	WAP12	-9.62	-83.58	-13.71	-99.71	0.16
July 2015	WAP15	-10.36	-85.10	-13.20	-95.62	0.09
July 2015	WAP20	-11.19	-92.49	-14.59	-106.74	0.10
July 2015	WAP21	-10.37	-88.83	-14.56	-106.46	0.14
July 2015	WAP23	-13.04	-105.32	-16.27	-120.12	0.07
July 2015	WAP24	-12.77	-103.15	-15.92	-117.34	0.08
July 2015	WAP25	-13.13	-105.93	-16.35	-120.79	0.07
July 2015	WAP26	-13.13	-107.15	-16.83	-124.62	0.09
July 2015	WAP27	-12.87	-106.47	-17.09	-126.73	0.10
July 2015	WAP32	-9.76	-87.69	-15.30	-112.41	0.21
July 2015	WAP33	-10.61	-90.59	-14.84	-108.72	0.14
July 2015	WAP34	-10.26	-91.04	-15.80	-116.40	0.19
July 2015	WAP37	-11.63	-96.96	-15.57	-114.59	0.11
July 2015	WAP39	-11.72	-95.93	-15.01	-110.06	0.09
Sept 2015	WAP05	-8.99	-76.48	-12.01	-86.08	0.13
Sept 2015	WAP07	-8.89	-75.44	-11.79	-84.33	0.12
Sept 2015	WAP12	-10.31	-82.44	-12.46	-89.66	0.07
Sept 2015	WAP15	-8.79	-73.57	-11.33	-80.64	0.11
Sept 2015	WAP20	-8.81	-75.72	-11.96	-85.69	0.14
Sept 2015	WAP21	-9.14	-78.15	-12.39	-89.09	0.13
Sept 2015	WAP23	-11.62	-96.69	-15.48	-113.84	0.11
Sept 2015	WAP24	-11.84	-96.80	-15.13	-111.00	0.09
Sept 2015	WAP25	-12.36	-100.04	-15.47	-113.73	0.08
Sept 2015	WAP26	-12.49	-100.20	-15.31	-112.48	0.07
Sept 2015	WAP27	-12.18	-99.51	-15.58	-114.61	0.09
Sept 2015	WAP32	-10.42	-85.07	-13.12	-94.96	0.09
Sept 2015	WAP33	-9.63	-83.58	-13.70	-99.58	0.15
Sept 2015	WAP34	-11.09	-89.95	-13.85	-100.78	0.08

Sept 2015	WAP37	-11.18	-90.94	-14.05	-102.42	0.08
Sept 2015	WAP39	-10.71	-89.06	-14.08	-102.64	0.11

E/I ratios that had negative values are not reported as the framework could not accurately represent these ponds.

Appendix B.

Evaporation pan water isotope composition

Date 2010	**$\delta^{18}O$‰**	**$\delta^{2}H$‰**	**Date 2011**	**$\delta^{18}O$‰**	**$\delta^{2}H$‰**
June 24	-10.9	-100.0	June 21	-10.8	-96.0
June 30	-8.6	-90.0	June 28	-8.6	-85.0
July 7	-7.7	-74.0	July 5	-6.3	-77.0
July 14	-6.4	-72.0	July 12	-4.4	-65.0
July 21	-4.4	-62.0	July 19	-5.3	-64.0
July 28	-5.4	-63.0	July 26	-4.7	-64.0
Aug 4	-6.3	-71.0	Aug 2	-6.2	-67.0
Aug 11	-5.0	-66.0	Aug 16	-6.9	-74.0
Aug 18	-8.1	-74.0	Aug 23	-8.2	-76.0
Aug 25	-10.3	-85.0	Aug 31	-8.7	-81.0
Sept 13	-9.13	-76.0	Sept 6	-8.4	-78.0
Sept 16	-9.0	-76.0	Sept 13	-8.19	-79.0
			Sept 22	-8.5	-76.0
Date 2012	**$\delta^{18}O$‰**	**$\delta^{2}H$‰**	**Date 2013**	**$\delta^{18}O$‰**	**$\delta^{2}H$‰**
June 20	-10.0	-99.9	June 28	-9.9	-95.6
June 27	-8.0	-91.5	July 3	-7.5	-84.5
July 4	-6.1	-80.8	July 5	-6.4	-79.3
July 11	-5.7	-79.3	July 12	-6.1	-74.5
July 18	-6.1	-45.9	July 19	-8.0	-81.9
Aug 8	-6.1	-19.3	July 26	-6.8	-76.9
Aug 9	-8.4	-107.6	Aug 2	-6.7	-71.3
Aug 16	-8.8	-94.0	Aug 9	-7.6	-73.1
Aug 22	-8.7	-89.0	Aug 17	-6.0	-66.7
Aug 30	-8.9	-75.5	Aug 23	-6.9	-73.8
Sept 6	-8.4	-73.7			
Sept 13	-8.9	-70.4			
Sept 19	-8.6	-72.6			
Date 2014	**$\delta^{18}O$‰**	**$\delta^{2}H$‰**	**Date 2015**	**$\delta^{18}O$‰**	**$\delta^{2}H$‰**
June 11	-10.4	-115.2	June 12	-10.5	-95.6

June 19	-10.2	-100.1	June 14	-9.7	-93.0
June 26	-7.7	-88.7	June 26	-8.0	-86.4
July 3	-6.1	-72.4	July 3	-6.0	-77.9
July 10	-6.2	-73.8	July 10	-10.3	-96.4
July 17	-7.8	-79.5	July 17	-7.6	-82.0
July 24	-7.8	-81.3	July 24	-7.5	-81.9
July 31	-7.0	-76.9	July 31	-6.9	-76.0
Aug 7	-6.9	-77.2	Aug 7	-5.7	-64.4
Aug 14	-7.4	-76.9	Aug 14	-5.3	-62.0
Aug 21	-7.5	-76.4	Aug 21	-5.4	-63.6
Aug 28	-7.1	-74.9	Aug 28	-5.3	-63.4
Sept 5	-7.4	-75.7	Sept 4	-6.0	-65.5
Sept 11	-8.8	-81.8	Sept 11	-5.0	-56.7
Sept 18	-9.7	-89.3	Sept 18	-6.6	-65.9
			Sept 25	-7.7	-71.6

Appendix C

Flux Weighted Temperatures and Humidity

Date 2010	**Temp**	**Rh (avg)**	***li***	***a***	***N***	***L***	***Et (tot)***	**Flux T**	**Flux rh**
June	5.5	76.0	1.15	0.53	30.0	21.30	449.78		
July	12.2	76.6	3.81	0.53	31.0	20.06	670.07		
August	10.5	83.3	3.04	0.53	31.0	17.07	526.39		
Sept	6.5	83.4	1.48	0.53	30.0	14.19	327.73		
Avg	8.6	80.5	2.37	0.53	30.5	18.16		9.27	80.39
Date 2011	**Temp**	**Rh (avg)**	***li***	***A***	***N***	***L***	***Et (tot)***	**Flux T**	**Flux rh**
June	7.7	76.5	1.91	0.55	30.0	21.29	467.14		
July	14.3	74.9	4.83	0.55	31.0	20.08	641.16		
August	12.9	83.7	4.14	0.55	31.0	17.10	515.67		
Sept	10.2	74.1	2.91	0.55	30.0	14.22	364.40		
Avg	11.2	77.3	3.45	0.55	30.5	18.17		11.63	77.41
Date 2012	**Temp**	**Rh (avg)**	***li***	***a***	***N***	***L***	***Et (tot)***	**Flux T**	**Flux rh**
June	6.5	78.5	1.48	0.54	30.0	21.31	436.89		
July	14.6	74.3	4.98	0.54	31.0	20.02	661.33		
August	13.1	77.5	4.24	0.54	31.0	17.02	529.98		
Sept	8.4	83.7	2.17	0.54	30.0	14.15	333.92		
Avg	10.6	78.5	3.22	0.54	30.5	18.12		11.33	77.69
Date 2013	**Temp**	**Rh (avg)**	***li***	***a***	***N***	***L***	***Et (tot)***	**Flux T**	**Flux rh**
June	10.1	63.3	2.87	0.55	30.0	21.31	540.90		
July	14.6	73.6	4.98	0.55	31.0	20.04	644.66		
August	12.2	79.3	3.81	0.55	31.0	17.05	496.54		
Sept	8.7	79.6	2.29	0.55	30.0	14.17	331.19		
Avg	11.4	73.9	3.49	0.55	30.5	18.14		11.82	73.22
Date 2014	**Temp**	**Rh (avg)**	***li***	***a***	***N***	***L***	***Et (tot)***	**Flux T**	**Flux rh**
June	9.8	67.6	2.74	0.54	30.0	21.30	550.94		

July	13.6	75.8	4.48	0.54	31.0	20.06	641.54		
August	12.6	77.4	4.00	0.54	31.0	17.07	523.68		
Sept	6.3	81.3	1.41	0.54	30.0	14.19	288.09		
Avg	10.5	75.5	3.16	0.54	30.5	18.15		11.24	74.75
Date 2015	**Temp**	**Rh (avg)**	***li***	***a***	***N***	***L***	***Et (tot)***	**Flux T**	**Flux rh**
June	7.8	78.3	1.95	0.53	30.0	21.29	521.37		
July	11.9	81.9	3.67	0.53	31.0	30.08	637.19		
August	10.9	85.3	3.24	0.53	31.0	17.09	518.57		
Sept	7.0	81.4	1.65	0.53	30.0	14.21	328.05		
Avg	9.4	81.7	2.63	0.53	30.5			9.79	81.79